

Integrated Masters in Bioengineering

*Three-dimensional Agent-based modelling of  
Quorum Sensing in Biofilms*

Master's Thesis

of

Gonçalo Filipe Cardoso Lamas

Developed within the discipline of Dissertation

Conducted at

LEPABE



FEUP advisor: **Dr Nuno Azevedo**  
U. Vigo Co-advisor: **Dr Anália Lourenço**

Department of Chemical Engineering

July of 2021





## Acknowledgements

Firstly, I would like to thank LEPABE (Laboratory for Process Engineering, Environment, Biotechnology and Energy). This work was financially supported by: base funding - UIDB/00511/2020 of Investigation Unit - Laboratory for Process Engineering, Environment, Biotechnology, and Energy – LEPABE - funded by national funds through FCT/MCTES (PIDDAC).

I am also extremely thankful to my advisor, Dr Nuno Azevedo for all the support and availability provided during the semester and for all the hours spent on calls guiding me through this thesis.

To my co-advisor, Dr Anália Lourenço, words cannot express my gratitude for all the time spent on helping me, the availability and quickness in response to everything, all the skype calls analysing the code that became moments were a good time was also had, due to all the laughs and conversations.

To Beatriz Magalhães all the thanks for the availability to help me and the quickness of response every time I had some question or even in giving feedback about the work.

I also need to thank the ones that kept me company while working on this thesis. Tufas and B, thanks for being there and making me laugh at your silliness and cuteness. I do not know what these last few years would be without you, especially during the quarantines.

As the acknowledgements cannot be restricted to the period this thesis was made but also to the amazing five years I had. I want to thank all the friends that made this journey something to remember for the rest of my life. A special thanks to the ones of the same year as me that accompanied me through all the good and bad. Ana Sofia, Luana, Rui, Rui, Tiago, Alexandre, Maria, Vitória, and Sofia, friends are the family the heart chooses and I could not be luckier to have you as family.

Not less important to me are the friends that gather to explore unknown worlds and fight incredible monsters, fighters, and sorcerers. Thank you for the good times and laughs, during and outside of these explorations, for all the friendship and kindness. Mari will always be available to be the service cleric.

To my kiwi business partners, thank you for all the random talks and the friendship we developed, during these past three years.

Lastly, but not least, I would like to thank my family, namely my mother and sister, for always being there for me and for all the support on everything.

To all these people, my sincere thank you for always believing in me and that I can always improve, do better and achieve my goals.

---

## Resumo

Os biofilmes são agregados de microrganismos que formam uma estrutura complexa e dinâmica com a ajuda de uma matriz constituída principalmente por exopolissacarídeos. Os biofilmes formam-se naturalmente e conseguem ajudar a metabolizar toxinas e poluentes ambientais. Eles também podem ser usados em tratamentos de águas residuais, filtração de águas e como biocatalisadores. Contudo, eles também podem causar infecções no ser humano, animais e plantas. Assim como causar *biofouling*, contaminação de águas processadas, deterioração de água potável e corrosão. Uma parte central da formação destas estruturas é o sistema de *quorum sensing* nos microrganismos. *Quorum sensing* é um sistema de sinalização químico que ajuda os organismos a comunicar entre si e a coordenarem-se. Esta comunicação acontece com a ajuda de pequenas moléculas, os indutores. Estes indutores estão divididos em três grupos: as acil-homoserina lactonas, os péptidos e os autoindutor-2.

Nesta tese, um modelo baseado em agentes foi otimizado e aplicado para melhor entender a comunicação entre organismos dentro de um biofilme. Foram focados os sistemas que usam péptidos e AI2 como indutores. No total sete fatores foram estudados: a distância entre células, a diferença nos resultados entre o modelo baseado em agentes e uma abordagem puramente matemática, a orientação do recetor, o tamanho do recetor, a alimentação de indutores vinda de fontes externas, a alimentação a partir das duas células em análise em simultâneo, e a evolução da concentração no meio com quatro células a libertar constantemente indutores.

A distâncias maiores não ocorre influência na absorção de indutores, sendo que esta absorção foi, sensivelmente, a mesma. A diferença maior entre os resultados dos modelos foi de 1.1 % em todos os casos testados. A comunicação regular entre organismos não pareceu ser afetada pela presença de outros tipos de alimentação, quer externa, quer do recetor. Um estado estacionário foi alcançado em todos os testes com quatro células a libertar indutores constantemente, este estado foi atingido entre 750 e 900  $\mu$ s. O modelo baseado em agentes mostrou ser uma ótima ferramenta para avaliar, a nível molecular, o impacto que fatores, como distâncias e orientação das células, têm na comunicação celular.

**Palavras Chave:**

Modelo baseado em agentes, *Quorum sensing*, Indutores peptídicos e AI2, Biofilmes.

---

## Abstract

Biofilms are aggregates of microorganisms, forming a complex and dynamic structure with the help of a matrix mainly constituted by exopolysaccharides. Biofilms form naturally and can help metabolize toxins and environmental pollution. Biofilms can also be applied on wastewater treatment, filtration of water, or as biocatalysts. However, biofilms also cause infections in humans, animals, and plants, as well as biofouling, contamination of process water, deterioration of potable water, and corrosion. A core part of the formation of these structures is the quorum sensing systems in the microorganisms. Quorum sensing is a chemical signalling system that helps microorganisms communicate and coordinate with each other. This communication happens with the help of small molecules, the autoinducers. These inducers fall into three groups: the acyl-homoserine lactones inducers, the peptide inducer, and the autoinducer-2.

In this thesis, an agent-based model was optimized and applied to better understand the communication between organisms inside a biofilm. The focus was on the peptide and AI2 inducers. In total seven factors were studied: the distances between cells, the difference in results between agent-based modelling and a purely mathematical approach, the orientation of the receptor, the size of the receptor, the feeding from external sources, the feeding from the two cells at the same time, and the evolution of concentration on the medium with constant release from four cells.

The studied distances between cells have little influence on the uptake of inducers. The maximum difference between results was a difference of 1.1 % in the uptake of the inducers in all the cases. The size of the receptor did not seem to affect the uptake of AIs, for both orientations tested. The regular communication between cells was not affected by the presence of other types of feeding, from external sources or from the receptor itself. A steady state was achieved on every test with four cells releasing inducers constantly, this state was achieved between 750 and 900  $\mu$ s. Agent-based modelling demonstrated to be a great tool to assess, on the molecular level, the impact that factors, like small distances and cell orientation, have on cellular communication.

**Keywords:** Agent-based modelling, Quorum sensing, Peptide and AI2 inducers, Biofilms.

---



## Declaration

I, Gonçalo Filipe Cardoso Lamas, declare, on my own honour, that this is an original work and that all information from outside sources is appropriately cited, with the identification of the source.

*Gonçalo Cardoso*

*Porto, 5 of July 2021*

---

*"I don't know anything about science other than that it's really good for you"*  
Екатерина Петровна Замолдчикова

---



# Index

<b>List of figures</b> .....	<b>iii</b>
<b>List of tables</b> .....	<b>v</b>
<b>Nomenclature</b> .....	<b>vi</b>
<b>1 Introduction</b> .....	<b>1</b>
1.1 Background and presentation of the project .....	1
1.2 Used technology.....	2
1.3 Structure of the document.....	3
<b>2 State of the Art</b> .....	<b>4</b>
2.1 Biofilms and Quorum Sensing .....	4
2.2 Agent-based modelling.....	9
<b>3 Technical Description</b> .....	<b>15</b>
3.1 Environment .....	15
3.2 Agents .....	16
3.2.1 Concentration .....	16
3.2.2 Hydrodynamic radius .....	17
3.2.3 Diffusion coefficient .....	17
3.2.4 Initial spatial location and movement direction .....	18
3.3 Rules.....	18
3.4 Quantification of Quorum Sensing mediation.....	19
3.5 Simulation settings.....	20
3.6 Simulations .....	20
3.7 Statistical Analysis.....	21
<b>4 Results and discussion</b> .....	<b>22</b>
<b>5 Conclusions</b> .....	<b>29</b>
<b>6 Limitations and Future Work</b> .....	<b>30</b>

**References..... 31**

**Annex..... 43**

## List of figures

Figure 1. Stages of formation of biofilm. (1) Cells adhere to the surface; (2) production and secretion of EPS molecules, beginning the formation of the matrix; (3) proliferation of the cells; (4) formation of a mature biofilm; (5) after reaching certain size microorganisms are released. Adapted from (Monroe, 2007). ..... 5

Figure 2. Scheme of a generic AHL QS system, from the detection to the production of new AI molecules. (Ganesh & Rai, 2018) ..... 6

Figure 3. Scheme of a generic peptide QS system, from the detection to the production of new AI molecules. (Ganesh & RAI, 2018)..... 6

Figure 4. Scheme of a generic AI2 QS system, from the detection to the production of new AI molecules. (Borges & Simões ,2019) ..... 7

Figure 5. Schematic example of peptide quorum sensing in *S. mutans*, since the uptake of the inducer to the respective response and release of more inducers. (Y. H. Li et al. 2002)..... 8

Figure 6. Brownian motion in a crowded environment. The movement occurs by collision with the surrounding agents. The green line shows an example of movement for the green dot. Addapted from Pérez-Rodríguez et al., 2018..... 17

Figure 7. Collision detection and resolution.  $V_1$  stands for the velocity of the agents before collision, while  $V_2$  is the velocity afterwards.  $\Theta$  is the deflection angle between the normal and the velocity of the agent (adapted from Pérez-Rodríguez et al., 2018). ..... 19

Figure 8. Schematic diagram of the spheric cell *S1* and the spherocylinder one *S2*, when they are perpendicular to each other. Only the spherical end of the bacillus was considered because that was the main part that was able to interact, through the AIs, with the coccus (left). Schematic diagram of the sphere cell and the spherocylinder one, when they are parallel to each other. Only the cylindric centre of the bacillus was considered because that was the main part that was able to interact, through the AIs, with the coccus (right)..... 19

Figure 9. Example of the position of the cells on tests between *S. mitis* and *P. aeruginosa*, when they are aligned horizontally (A), and *S. mitis* and *S. mutans* (B), both at  $5 \mu\text{m}$ . ..... 20

Figure 10. Example of the environment feeding test between *S. mitis* and *P. aeruginosa*, when they are aligned horizontally, at  $5 \mu\text{m}$  (A). Example of the dual feeding test between *S. mitis* and *P. aeruginosa*, when they are aligned horizontally, at  $5 \mu\text{m}$  (B). Example of the test between several *S. mitis* positioned randomly (C). ..... 21

Figure 11. Distribution of AIs on the different octants of the releaser cells of each shape (*S. mitis* – A; *P. aeruginosa* – B). The grey numbers represent the number of AIs released on the back octants, while the black represents the ones released on the front octants. .... 22

Figure 12. Results for the algebraic approach and simulation tests of *P. aeruginosa* and *S. mitis* (above) *S. mutans* and *S. mitis* (below) at different distances, where the former of each duo is the one releasing the sensor molecule. .... 23

Figure 13. Average time a molecule took to be absorbed by the receptor cell for each of the distances tested, for the duo *S. mitis* and *P. aeruginosa*, aligned horizontally. .... 24

Figure 14. Example of the position of the cells on a test between *S. mitis* and *P. aeruginosa*, when they are aligned vertically, at 5  $\mu\text{m}$ . .... 24

Figure 15. Results for the simulation tests of *S. mitis* and *P. aeruginosa* aligned vertically at different distances, where the former is the one releasing the sensor molecule ..... 25

Figure 16. Results for the simulation tests of *S. mitis* and *P. aeruginosa* aligned horizontally (A) and vertically (B) for different length values of the *P. aeruginosa*, where the former is the one releasing the sensor molecule. .... 25

Figure 17. Results of the simulations tests of an additional environmental feeding compared to feeding from only a single cell. .... 26

Figure 18. Results of the simulations tests of feeding from both cells compared to feeding from a single cell..... 27

Figure 19. Results of the simulations with four *S. mitis* randomly positioned. .... 27

## List of tables

*Table 1. Review on microorganisms, their morphology and quorum sensing systems ..... 12*

*Table 2. The characteristics of a generic agent-based model defined for quorum sensing..... 15*

*Table 3. Basic agent properties and interaction rules in the QS simulations..... 16*

*Table 4. Cells used and their autoinducer, dimensions and volume. .... 16*

*Table 5. AI molecular weight, radius, and diffusion coefficient for the ABM model ..... 18*

## Nomenclature

<i>ABM</i>	<i>Agent-based modelling</i>
<i>AHL</i>	<i>Acyl-homoserine lactones</i>
<i>AI</i>	<i>Autoinducer</i>
<i>AI2</i>	<i>Autoinducer-2</i>
<i>CSP</i>	<i>Competence stimulating peptide</i>
<i>EPS</i>	<i>Exopolysaccharides</i>
<i>MASON</i>	<i>Multi-agent simulator of neighbourhoods</i>
<i>QS</i>	<i>Quorum sensing</i>

# 1 Introduction

## *1.1 Background and presentation of the project*

Biofilms are multicellular structures that are widely distributed around Earth (Stoodley et al., 2002). Usually, they have a negative connotation due to infection in humans (for instance in medical devices), animals and plants (Costerton et al., 1987; Shirtliff & Leid, 2009), and other problems like biofouling, contamination of process water, deterioration of potable water and corrosion (Fleming et al., 2011; Little & Lee, 2014; Wingender & Flemming, 2011). However, biofilms can also have a positive impact. This impact is important for the ecological balance since it helps the bioremediation of the soil and sediments, by metabolizing toxins, that planktonic cells would be too sensitive to metabolize. It also helps to degrade environmental pollution, where constituents of the matrix help the solubilization of hydrophobic or recalcitrant substrates that were, otherwise, inaccessible to microorganisms (M. K. Yadav, 2018). Some other benefits include biotechnological applications including filtration of water, degradation of wastewater and its solid waste, and as biocatalysts (Halan et al., 2012). Therefore, understanding biofilms, their dynamic and complex structures, as well as their mechanisms will allow their prevention when unwanted and enhance their growth when desirable. One of the mechanisms present in this cellular aggregate of microorganisms is the intra and interspecies communication between the cells in a biofilm. The communication happens with the help of small molecules, denominated autoinducers (AI), which are part of a chemical signalling system denominated quorum sensing (QS) (Sturbelle et al., 2015).

Sometimes, *in vivo* and *in vitro* experiments can be too costly, impossible to carry out with the available technology, or when, due to its complexity, the problem averts analytical resolution (Castiglione, 2009). One example of these experiments is the evaluation of the position of certain molecules over time. A possible way of studying biological environments that are impractical to investigate in the wet lab is through *in silico* experiments. For example, *in vitro* experiments may evaluate the impact on the variation of a specific parameter when applied to a molecule. However, this requires tracking the position of that molecule on a nano time scale, which makes these experimental methods very time consuming (McGuffee & Elcock, 2010). In comparison, the ease of working with when compared to *in vitro* and *in vivo* experiments and the elucidation given by *in silico* testing on the interactions between molecules and microorganisms makes this method appealing. Moreover, it saves money and sometimes time, by reducing the number of *in vitro* and *in vivo* tests done.

The application of *in silico* models to the biological world implies knowledge about the spatial distributions, concentrations, and reaction rates of the entities that constitute the system under study. Such data is not always available, which brings forward the need of using mathematical abstraction (Kollmann & Sourjik, 2007). Some challenges are met with the design of large models, among them are the incorporation of the scales of time and space on different orders of magnitude (Pérez-Rodríguez et al., 2016). To avoid high computational costs, the models tend to be simplified. For example, instead of representing the whole environment that occurs in the real world, only part of it is considered. Such is the case of the work by Pérez-Rodríguez, where the biofilm was only represented by a couple of cells (Pérez-Rodríguez et al., 2018).

Models can be divided into two types, especially when applied to the biological world, the fine-grained and the coarse-grained models. The former uses atomistic details (Christen & Van Gunsteren, 2006). The latter, instead of focusing on the atoms, focus on molecular systems and interaction sites, eliminating details considered non-essential (Noid, 2013). Traditionally, this type of *in silico* model follows two approaches, even though there is a third one less common, the middle out. The first one is called top-down, in which system-level patterns and features are analysed to direct the design of the models. The other one is the bottom-up approach, where the study of several system components is done to merge the observations into models able to predict the system's behaviour. The latter englobes agent-based modelling (ABM), a model that looks at the behaviour of the individuals, called agents, to construct the overall picture of the system's behaviour. The system is, thus, represented as a collection of these agents and their actions.

This project aims to employ a coarse-grained model, ABM, on well-characterized bacterial biofilms to better understand the influence of several factors, namely distance, cell size, environment influence and others, on their communication. Simulations cover microorganisms relevant to the formation of multispecies biofilms, so a better understanding of their formation and maintenance can be achieved. These microorganisms are *P. aeruginosa*, *S. mutans* and *S. mitis*. This goal entailed: research of well-characterized QS mechanisms; investigation of the organisms where such QS occurs and analyse their structural properties, as well as of their chemical signals; definition of the pairs of species that will be studied together according to the previous research; quantification of the QS mediation of such pair; optimization of the model; simulation of the intended experiments and analysis of its results.

## 1.2 Used technology

To simulate the intended experiments, the open-source Java framework multi-agent simulator of neighbourhoods (MASON) was used (Luke et al., 2005). This program was developed with special attention to simulations of many agents, even though it is flexible to be used on a wide range of simple



experiments. Its applications are many, including network intrusion and countermeasures; urban traffic simulation; ant foraging; and anthrax propagation on the human body (Luke et al., 2005).

MASON is built upon three layers: the utility, the model, and the visualization layers. The former embodies classes, such as random number generator and movie and snapshot-generating facilities, that can be used for any purpose. The model layer consists of a small collection of classes that involve a discrete event schedule and a variety of fields that associate objects with their locations. To write basic simulations that run on the command line, this layer's code is enough. The former is responsible for visualizing and manipulating the model. It is related to the model layer, in the sense that, for most elements in the model layer exists an equivalent element in the visualization layer, that will manipulate the model object, picture it and analyse the contents (Luke et al., 2005).

When compared to other multiagent simulators like Ascape, RePast and SWARM, they all offer graphical visualization, stochastic event ordering, generation of different forms of media and inspection of the objects (Luke et al., 2005). However, MASON also provides visualization of 2D and 3D fields in a 3D environment and a more sophisticated and flexible visualization of 2D. It is also faster both in the model and in the visualization, planned to be able to produce duplicable results (Luke et al., 2005).

### *1.3 Structure of the document*

This document is organized into 6 chapters, as follows:

1. Introduction: description of the contextualization of the project relevance and theme, as well as the goals intended to achieve, and the technology used to complete it.
2. State of the Art: a review of the most relevant topics to this thesis, including the quorum sensing systems and agent-based modelling.
3. Technical description: presentation of the main programming for the modelling of the computational agents and the tests performed to validate simulation outputs.
4. Results and discussion: discussion of the obtained results.
5. Conclusion: analysis of the major results of the thesis.
6. Limitations and Future Work: points out the limitations of the present work and proposes future research directions.

## 2 State of the Art

### *2.1 Biofilms and Quorum Sensing*

Biofilms are dynamic and complex structures, made up of cellular aggregates of microorganisms (Donlan, 2001), having a range of  $10^8$  to  $10^{11}$  cells per gram of wet weight of the biofilm. These biofilms can have only one species or multiple species of microorganisms (Balzer et al., 2010, Morgan-Sagastume et al., 2008 in Flemming et al., 2016). They are called aggregates since the cells in biofilm often experience cell-to-cell contact, whether if they are surface-attached biofilms or in flocs. The former happens when one layer of the cells is in direct contact with a surface, also known as substratum, while the latter are mobile biofilms that occur without the presence of the substratum (Hans Curt Flemming et al., 2016).

The adhesion, either to each other or the surface, is through substances produced by the microorganism itself, namely extrapolymeric substances (EPS), that will guarantee cohesion and adhesion, forming a matrix (Halan et al., 2012). The formation of this matrix is essential and depends on nutrient availability, shear stress and social competition. It is crucial since they have a structural and physicochemical centrality on the biofilm, even though its energetic cost is high. It will confer spatial organization, from which the biofilm acquires steep gradients, biodiversity and interaction like cell-to-cell communication and enhanced horizontal gene transfer (Hans Curt Flemming et al., 2016). For instance, amyloid fibers show a weak, but functional affinity to the molecules responsible for intercellular communication, which provides a mechanism that modifies the concentration of such molecules in the matrix (Seviour et al., 2015). This will allow signalling molecules to be restricted, in order to achieve the needed concentration to be sensed (Redfield, 2002). The local conditions provided by the matrix and the coordination of life cycles, given by the communication, can trigger the cells to differentiate (Singer et al., 2010 in Flemming et al., 2016).

Due to their nature, biofilms have some properties that cannot be found on cells in suspension, also known as planktonic cells. They are self-regenerating, spatially and metabolically organized, due to their differentiation, and are more resistant to toxic substrates and products, because of the enhanced rates of gene exchange and of the EPS matrix that encases the cells (Flemming & Wingender, 2010 in Flemming et al., 2016; Halan et al., 2012).

The formation of biofilms is a complex process (Figure 1) and is affected by plenty of factors, including cellular, surface-related, and environmental (Halan et al., 2012).

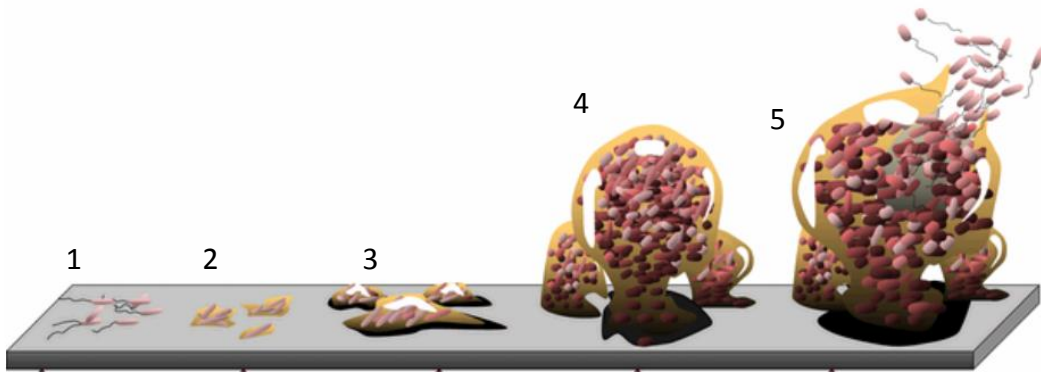


**Figure 1.** Stages of formation of biofilm. (1) Cells adhere to the surface; (2) production and secretion of EPS molecules, beginning the formation of the matrix; (3) proliferation of the cells; (4) formation of a mature biofilm; (5) after reaching certain size microorganisms are released. Adapted from (Monroe, 2007).

Firstly, the substratum needs to be conditioned by macromolecules, so a nutritious zone is formed where the cells can settle. Planktonic cells, eventually, start to interact with said surface, attaching to it, either reversibly or irreversibly, through flagellar motility, surface translocation, twitching, gliding, and sliding (Halan et al., 2012) (Figure 1-1). When the cells are irreversibly attached, they start to reproduce and secrete EPS molecules, that will link to each other and the cell (Halan et al., 2012) (Figure 1-2). The biofilm will start to develop (Figure 1-3) and mature, forming a complex architecture with channels and pores built within. They will allow water and nutrients to diffuse through the several layers of the biofilm, as well as release unwanted and waste substances (Figure 1-4). A near steady-state is settled when the thickness is kept stable by the detachment of cells from the biofilm and its regrowth (Halan et al., 2012) (Figure 1-5).

A core part of the formation and maintenance of the biofilm is the QS system, which consists, as previously mentioned, of a system of chemical signalling that depends on cell density. In these systems, cells release small molecules, denominated AIs, to the medium, which will promote inter and intraspecies communication. This will allow bacteria to communicate and coordinate their behaviour and function simulating a multicellular organism, controlling, as well, the expression of genes during the formation and maturation of the biofilm. Whenever the AI reaches a high concentration, the molecule will interact with regulatory proteins that module genic expression (Sturbelle et al., 2015). There are 3 main systems of QS in microorganisms that use AIs: acyl-homoserine lactones (AHLs), peptides, and autoinducers 2 (AI2). The first two are present in Gram-negative and Gram-positive bacteria, respectively, while the third can be found on both (M. B. Miller & Bassler, 2001).

In the first-mentioned QS, the signal is an acylated homoserine lactone that can diffuse through the cell membrane (Figure 2). The ring on this molecule is conserved on all signals identified so far, however, the acyl side chain may vary in length, degree, and type of replacement. Two structural

genes are necessary, the one that codes for AHL synthase and the one that codes for the response regulator of such molecule. Usually, these synthases belong to the LuxI family (Sharma et al., 2016). When the signal levels increase, due to a rise in local cell density or areas of restrictive local diffusion, the signal interacts with a protein coded by a gene from the LuxR family. The complex signal-LuxR homologous modules the gene expression regulated for QS (J. Engebrecht et al., 1983; J. A. Engebrecht & Silverman, 1984; J. Engebrecht & Silverman, 1987). Several LuxI and LuxR counterparts are found in a wide variety of Gram-negative bacteria, and they control several processes that encompass virulence and biofilm formation (Sharma et al., 2016).

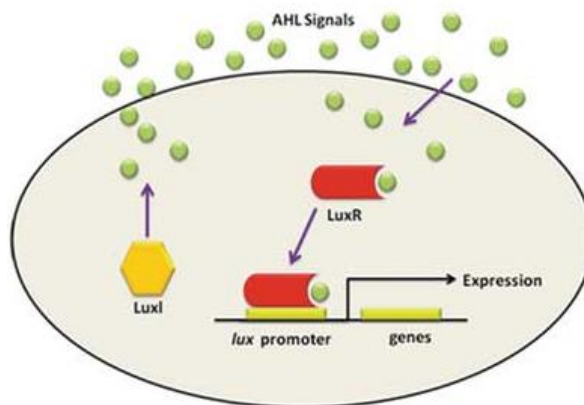


**Figure 2.** Scheme of a generic AHL QS system, from the detection to the production of new AI molecules. (Ganesh & Rai, 2018)

Signalling based on peptides usually involves the production of small peptides, either linear or cyclic, that are translated as a bigger pro-peptide inside the cell, and then processed during secretion (Figure 3). Contrasting AHL QS, peptide signals are not detected inside the cell. A sensor protein, connected to the cell membrane, belonging to the two-component signal transduction family, interacts with the peptide. The sensor, when connecting to the peptide, activates a cascade mechanism of phosphorylation/dephosphorylation, that will modulate the gene expression regulated by the QS. This

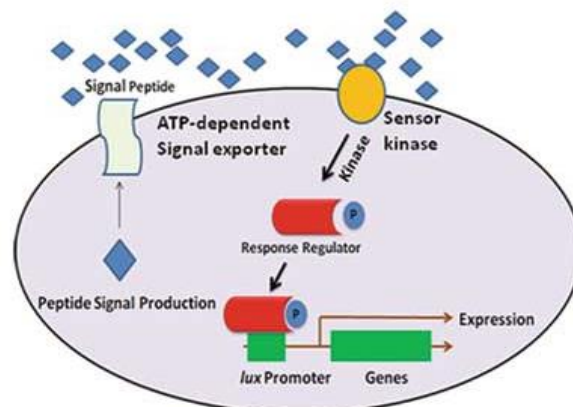


**Figure 3.** Scheme of a generic peptide QS system, from the detection to the production of new AI molecules. (Ganesh & RAI, 2018)

series of phosphoryl events culminates in the phosphorylation of a cognate response regulator protein, which will allow it to bind to the DNA and alter the transcription of the genes to the target genes (M. B. Miller & Bassler, 2001).

The latter QS allows bacteria to communicate inter and intraspecies (Figure 4). This notion emerged with the discovery and study of the AI<sub>2</sub>, which is one of the signals used by *V. harveyi* on the QS. Specifically, LuxS that codes the AI<sub>2</sub> synthase is present on about half of all the bacterial genomes sequenced, the production of this molecule was verified on an elevated number of these species, and AI<sub>2</sub> controls the gene expression in a variety of them (Waters & Bassler, 2005). LuxS product is a molecule called 4,5-dihydroxy-2,3-pentanedione (DPD) that undergoes cyclization and hydration to form either r-thmf or s-thmf. The latter will convert into s-thmf-borate in the presence of boron (Pereira et al., 2013). However, other AI<sub>2</sub> derivatives may exist and be biologically active. These molecules and the respective receptors are not exclusive to a species. Some bacteria have shown to possess two or more AI<sub>2</sub> receptors in order to recognize the different derivatives of DPD and alter particular behaviours to the information conveyed by each signal. Since only the enzyme LuxS is required for the synthesis of these signalling molecules, the pathway may represent an economical method for a complex lexicon (Waters & Bassler, 2005). Just like peptide-based QS, the receptor activation will start a cascade effect of phosphorylation/dephosphorylation, that will control the downstream AI<sub>2</sub> quorum sensing regulon (Pereira et al., 2013).

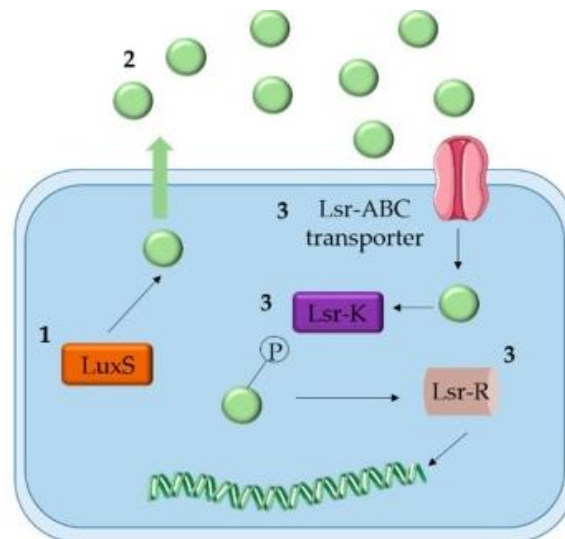


**Figure 4.** Scheme of a generic AI<sub>2</sub> QS system, from the detection to the production of new AI molecules. (Borges & Simões, 2019)

Several studies are reporting QS on bacteria, as can be seen in Table 1, where the focus was on the three main types of QS, even though other types may exist on the present bacteria. Two of the better described QS systems are the ones of *Pseudomonas aeruginosa* and *Streptococcus mutans*. These organisms do not seem to share a QS mechanism, *S. mutans* uses peptides as their AI, and the other

bases their system on AHL or AI2 molecules. However, *P. aeruginosa* can only uptake AI2 and not produce it (Z. Wang et al., 2016). One species shares a QS system with both these molecules, *Streptococcus mitis*. This organism has peptide and AI2 based QS systems, being able to uptake and produce both AIs (Salvadori et al., 2018; Z. Wang et al., 2016). Biofilms of *P. aeruginosa* and *S. mitis* can be found in the upper respiratory tract of infants. *S. mitis* is also commonly found on the oral cavities along with *S. mutans* and both are early colonizers of dental multispecies biofilms, with *S. mutans* being a primary causative agent involved in dental caries in humans (Senadheera & Cvitkovitch, 2008; P. Yadav et al., 2020). The AI2 produced by *S. mitis* influences the behaviour of *P. aeruginosa* (Z. Wang et al., 2016).

Starting with *S. mutans*, its QS is very similar to the closely related species *Streptococcus pneumoniae*. It uses a 17-residue cationic peptide, the competence stimulating peptide (CSP), as the inducer. Its precursor gene is the *comC*, which belongs to the *comCDE* tricistronic operon, which also translates the membrane-bound histidine kinase sensor protein ComD, and its cognate response regulator ComE (Senadheera & Cvitkovitch, 2008). Besides this genetic loci, *S. mutans* also has the *comAB* genes that encode the secretion apparatus required for the process and exportation of CSP. Namely, ComA is an ATP-binding cassette transporter that will use COMB as the processor of the CSP precursor. When the ComD absorbs the AI, after a threshold concentration, it will be activated and go through autophosphorylation at a conserved histidine residue. This will result in the activation of the responder protein ComE, which will be followed by the transcription of *comAB* and *comCDE*, as well as an alternative sigma-factor, called *comX*, as can be seen in Figure 5. This creates a positive feedback loop that spreads competence among nearby cells (Salvadori et al., 2018). The activation of ComX will promote cell lysis and the release of DNA from a subfraction of the bacterial population (Senadheera & Cvitkovitch, 2008). This means that it may interfere with the formation of the biofilm (P. Yadav et al., 2020).

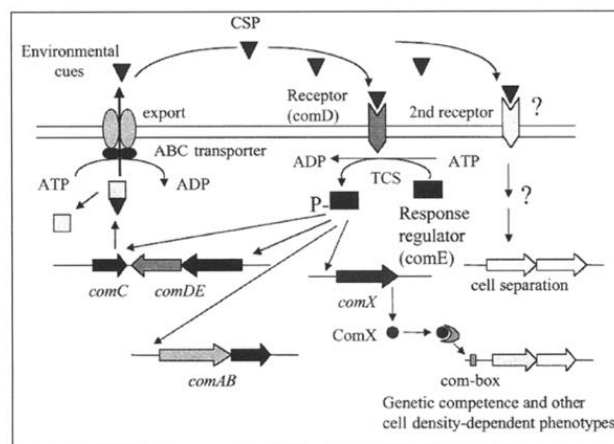


**Figure 5.** Schematic example of peptide quorum sensing in *S. mutans*, since the uptake of the inducer to the respective response and release of more inducers. (Y. H. Li et al. 2002)

Concerning *S. mitis*, the CSP regulatory system seems to be similar to that of *S. mutans* and *S. pneumoniae* strains, besides some other novel genes, whose functions still need elucidation (Salvadori et al., 2018). It is also known that this strain is able to produce AI2, which is encoded by the LuxS gene (Z. Wang et al., 2016). The LuxS system on the *S. mitis* is yet to be described (P. Yadav et al., 2020), however it was found that it can regulate the behaviour of *P. aeruginosa*, enhancing its adhesion and biofilm formation as well as alleviate the immune response induced by it (Song et al., 2015). Even though *S. mitis* is considered non-pathogenic, this proves that they should not be ignored (Song et al., 2015).

Considering *P. aeruginosa*, the main QS system involves AHL as their AI, but since the study will focus on the AI2 system, the AHL one will not be described. The AI2 system for *P. aeruginosa* is also not yet described, but it is known that it can uptake this molecule, which will enhance the biofilm formation, bacterial viability, and production of virulence factors. However, after a certain threshold, it will reduce these factors, meaning that at higher concentrations it downregulates the genes (H. Li et al., 2015).

## 2.2 Agent-based modelling

ABM is considered a more natural method for simulating real-world entities on a system, being more akin to reality than other methods (Gilbert & Terna, 2000). The origin of ABM could be traced to the work developed by Craig Reynolds in 1987, even though the true origins of the methodology are seldom identifiable in an ambiguous manner and some key concepts can be found earlier (Bodine et al., 2020; Reynolds, 1987). The aforementioned author studied the bird flock formation, considering only three rules of behaviour, which were to avoid collisions, try to match its velocity to the velocity of nearby agents and try to stay close to the other agents. These simple rules were able to create a model that recreates a realistic flocking behaviour (Bodine et al., 2020; Reynolds, 1987). Nowadays there are an array of other applications, including social, economic, ecological, physical, robotic, and traffic systems, with the intent of either analysing, predicting or verifying the proposed problem or theory (Davidsson et al., 2007).

ABM is a simulation tool in which “system-level (macro) behaviour is generated by the (micro) behaviour of the individual agents” (Bodine et al., 2020). That is, the system is defined as a collection of agents that are programmed to simulate a given behaviour. An ABM is composed of three different components: the agents, the rules, and the environment. The agents represent individual components of the system and behave as a single object obeying a set of rules that represent the key features of the system. The interactions of the agents with each other and with the environment will assemble complex behaviours of the whole system, that would not be observable on individual terms (J. Miller

et al., 2010). These interactions, either directly or indirectly, will help validate the various behaviours entailed in the model (Pérez-Rodríguez et al., 2015).

Important features of the agents include autonomy, heterogeneity, and intuition. They are free to interact with other agents without compromising their autonomy and are capable of processing information or exchange it with others, so independent decisions can be made. Agents are autonomous individuals, meaning that each agent can be different from the rest and, even though groups of agents can exist, they are formed from the bottom-up, becoming a group of similar agents. Their activity has a range of distinctive features, most notably: pro-active/goal-directed (i.e. agents have a goal to achieve), reactive/perceptive (i.e. agents are designed to have awareness of their surroundings), interactive/communicative (i.e. agents can communicate with each other), mobility and adaptation/learning (i.e. agents can be designed to alter their state depending on the previous states, and to adapt depending on the situation) ((Epstein & Axtell, 1997; Franklin & Graesser, 1996; Macal & North, 2010; Wooldridge & Jennings, 1995) in Crooks & Heppenstall, 2012).

The main advantages of ABM are the ability to capture emergent phenomena, provide an environment that simulates the natural world and flexibility (Crooks & Heppenstall, 2012). Its usefulness can be captured on some conditions. It is important to underline those where the interaction between agents is complicated, non-linear, discontinuous or discrete; there is a heterogeneous population of agents; where the topology of the interactions is heterogeneous and complex; and, where the behaviour of the agents is complex, namely learning and adaptation (Bonabeau, 2002). System dynamics can also be incorporated into the model. Even though time is still a discrete variable in the system, time steps can be made small enough to approximate real-time dynamics (Crooks & Heppenstall, 2012).

The most common goals involve elucidating and explaining behaviours of a system and the inference of certain rules on those behaviours. Yet, flexibility one of the model biggest appeals represents a challenge. This is because any number of rules can be applied to the agents and the environment, which can either be extremely simple or complex. For instance, gradients or patches programmed differently (Bodine et al., 2020).

Single-molecule modelling raises issues about the inaccurate representation of the system and high computational costs (Feig & Sugita, 2013). Even though the volume of experimental data is increasing, source experiments are heterogeneous causing the data integration to not be straightforward. For example, the use of enzyme kinetic data determined on studies with different temperatures or even strains (Gameiro et al., 2016).

To the best of the author's knowledge, the only work found so far on the application of ABM in QS was conducted by Pérez-Rodríguez et al. 2018, in which the diffusion of AHLs was analysed in an



environment of *P. aeruginosa* and *Candida albicans*. However, no work could be found about the other QS mechanisms using ABM.

**Table 1.** Review on microorganisms, their morphology and quorum sensing systems

Microorganism	Size	Morphology	QS communication	QS molecule	References
<i>Aeromonas hydrophila</i>	0.3-1.0 $\mu\text{m}$ x 1.0-3.5 $\mu\text{m}$	Bacillus	AHL	C4-AHL	(Horneman et al., 2007; Lynch et al., 2002; Simmons & Gibson, 2012)
<i>Aggregatibacter actinomycetemcomitans</i>	0.5–0.8 $\mu\text{m}$ x 0.6–1.4 $\mu\text{m}$	Coccobacillus	AI2	AI2 + receter rbsB	(Pereira et al., 2013; Rubin, 2018; “Subgingival Microbes,” 2015)
<i>Agrobacterium tumefaciens</i>	1.5-3.0 $\mu\text{m}$ x 0.6-1.0 $\mu\text{m}$	Bacillus	AHL	N-(3-oxooctanoyl)-AHL	(Caruso & Ramsdell, 2014; M. B. Miller & Bassler, 2001; Smith & Townsend, 1907; Szenthe & Page, 2003)
<i>Bacillus cereus</i>	1 $\mu\text{m}$ x 3-4 $\mu\text{m}$	Bacillus	AI2	AI2	( <i>ASAE Homepage</i> , n.d.; Pereira et al., 2013; Vilain et al., 2006)
<i>Bacillus subtilis</i>	0.25–1.0 $\mu\text{m}$ x 4-10 $\mu\text{m}$	Bacillus	Peptides	ComX, competence and sporulation factor	(Lu et al., 2018; M. B. Miller & Bassler, 2001; Yu et al., 2014)
<i>Borrelia burgdorferi</i>	1 $\mu\text{m}$ x 10-25 $\mu\text{m}$	Helical	AI2	n.i.	(Pereira et al., 2013)
<i>Burkholderia cepacia</i>	n.i.	Bacillus	AHL	C8-AHL	(B. Huber et al., 2001; Birgit Huber et al., 2002; S. C. M. Miller et al., 2002)
<i>Chromobacterium violaceum</i>	0.5-1 $\mu\text{m}$ x 2-3 $\mu\text{m}$	Coccobacillus	AHL	C8-AHL, C6-AHL	(Ray et al., 2004; Rekha et al., 2011)
<i>Dinoroseobacter shibae</i>	0.3–0.7 $\mu\text{m}$ x 0.3–1.0 $\mu\text{m}$	Coccobacillus or Coccus	AHL	C18:2-AHL; C18:1-AHL	(Biebl et al., 2005; Neumann et al., 2013; Zan et al., 2014)
<i>Erwinia carotovora</i>	0.5 $\mu\text{m}$ x 1.8 $\mu\text{m}$	Bacillus	AHL	3O-C6-AHL	( <i>Microbiology Society Homepage</i> , n.d.; M. B. Miller & Bassler, 2001; Perombelon & Michael, 1992)
<i>Escherichia coli</i>	0.5 $\mu\text{m}$ x 2 $\mu\text{m}$	Bacillus	AI2	AI2	(Antunes et al., 2010; <i>ASAE Homepage</i> , n.d.; <i>Britannica Homepage</i> , n.d.; Pereira et al., 2013)

<i>Haemophilus influenzae</i>	1 µm x 0.3 µm	Cocci	AI2	receptor RbsB	(Kuhnert & Christensen, 2008; Pereira et al., 2013)
<i>Helicobacter pylori</i>	0.5-1 µm x 2-4 µm	Helical	AI2	n.i.	(Kusters et al., 2006; O'Rourke & Bode, 2014; Pereira et al., 2013)
<i>Klebsiella pneumoniae</i>	0.5 µm x 2.506±0.131 µm	Bacillus	AI2	AI2	(Chen et al., 2020; Lenchenko et al., 2020; L. Liu et al., 2020)
<i>Moraxella catarrhalis</i>	0.6–1.0 µm	Diplococci	AI2	n.i.	(CDC Homepage, n.d.; Embers et al., 2011; Pereira et al., 2013)
<i>Mycobacterium avium</i>	n.i.	Bacillus	AI2	n.i.	(Pereira et al., 2013)
<i>Pseudomonas aeruginosa</i>	0.5-0.8 µm x 1.5-3 µm	Bacillus	AI2 AHL	AI2 3-OH-C12-AHL, C4-AHL	(Antunes et al., 2010; Cruz et al., 2020; Davies et al., 1998; De Kievit, 2009; Hultqvist et al., 2018; Iglewski, 1996; MR & EP, 2005; Pereira et al., 2013; Shin et al., 2019; Zhang et al., 2020)
<i>Pseudomonas putida</i>	0.5-0.6 µm x 4-1.7 µm	Bacillus	AHL	3-OH-C12-AHL	(Fekete et al., 2010; Hwang et al., 2009; Steidle et al., 2002)
<i>Rhodopseudomonas palustris</i>	0.4-1 µm x 1.5-3 µm	Bacillus	AI2	AI2	(Larimer et al., 2004; <i>Microbiology Society Homepage</i> , n.d.; Zhang et al., 2020)
<i>Ruegeria sp</i>	0.6–1.6 µm x 1.0–4.0 µm	Bacillus	AHL	3-OH-C14-AHL, 3-OH-C14:1-AHL, 3-OH-C12-AHL	(Garrity et al., 2005; Zan et al., 2014)
<i>Salmonella enterica ssp. enterica serovar Typhimurium</i>	0.7–1.5 µm x 2.2–5.0 µm	Bacillus	AI2	AI2	(Ethelberg et al., 2014; Murray et al., 2009; Pereira et al., 2013)
<i>Sinorhizobium meliloti</i>	n.i.	Bacillus	AI2	AI2	(Cheng et al., 2007; Pereira et al., 2013)
<i>Staphylococcus aureus</i>	0.5-1 µm	Coccus	Peptide	autoinducing peptide	

<i>Streptococcus mitis</i>	0.6-0.8 $\mu\text{m}$	Coccus	Peptide	CSP	(Antunes et al., 2010; Harris et al., 2002; Le & Otto, 2015; M. B. Miller & Bassler, 2001; Zhou & Yuqing, 2015) (Salvadori et al., 2018; Z. Wang et al., 2016; Zhou & Yuqing, 2015)
<i>Streptococcus mutans</i>	0.5-1 $\mu\text{m}$	Coccus	Peptide	CSP	(Bikash et al., 2018; Bikash & Tal-Gan, 2019; Krzyściak et al., 2017; Y. H. Li et al., 2002; Merritt et al., 2003; Ryan & Ray, 2003)
<i>Streptococcus pneumoniae</i>	0.5-1.25 $\mu\text{m}$	Coccus	Peptide	CSP	(M. B. Miller & Bassler, 2001; Ryan & Ray, 2003; Todar, 2003; Yang & Tal-Gan, 2019)
<i>Streptococcus suis</i>	1 mm	Coccus	AI2	AI2	(B. Liu et al., 2020; Y. Wang et al., 2014)
<i>Vibrio cholerae</i>	0.5-0.8 $\mu\text{m}$ x 1-3 $\mu\text{m}$	Bacillus	AI2	n.i.	( <i>ASAE Homepage</i> , n.d.; <i>MEDSCAPE Homepage</i> , n.d.; Pereira et al., 2013)
<i>Vibrio fischeri</i>	0.8-1.3 $\mu\text{m}$ x 1.8-2.4 $\mu\text{m}$	Bacillus	AHL	3O-C6-AHL	( <i>ASAE Homepage</i> , n.d.; Lazdunski et al., 2004; Madigan et al., 2015; M. B. Miller & Bassler, 2001; Rao et al., 2008)
<i>Vibrio harveyi</i>	n.i.	Bacillus	AI2	AI2	( <i>ASAE Homepage</i> , n.d.; Pereira et al., 2013)

### 3 Technical Description

The lack of studies on the peptide and AI2 QS mechanisms makes an interesting approach to take on this thesis. These two types of communication were modelled, so a better knowledge on these QS mechanisms can be achieved, as well as how the different molecules affect the different parameters. The cells in the simulations will be *S. mutans* and *P. aeruginosa*, each of them paired with *S. mitis*. These pairs will allow the study of both systems, peptide and AI2 QS, since *S. mutans* has the peptide QS system, *P. aeruginosa* responds to the AI2 one and *S. mitis* has both.

For the characterization of the ABM, it is essential to identify and define the environment, agents, and rules. The components for a generic ABM for QS, as well as the biological characterization needed for each of them, are defined in Table 2.

For the construction of the model, several assumptions were made to simplify it. Particularly, the viscosity of the medium was considered an approximation to the value of the water at 30 °C, other molecules that may be present on the extracellular medium were not considered, the AIs were represented based on a spherical approximation, size of the AI molecules was considered constant during time, the AIs can diffuse through the membrane easily and are detected inside the cell, only two types of cells were contemplated for each biofilm, the cells were also considered non-motile and their size was constant during time, the behaviour of the agents is the same on every section of the biofilm.

**Table 2.** The characteristics of a generic agent-based model defined for quorum sensing.

Generic agent-based model	Generic agent-based model for quorum sensing
Environment	Biofilm matrix
Agents	Cells Molecules (inducers)
Rules	Medium diffusion, interactions between agents

#### 3.1 Environment

To simplify, a subvolume of the biofilm where the QS takes place was simulated. However, this subvolume had to be sufficiently large to accommodate the matrix and the agents (cells and inducers). The boundaries within which the agents are contained are affected by the volume and orientation of the cells being tested. The environment was defined as a rectangular cuboid, large enough to fit the cells with a defined distance between them and a 0.1  $\mu\text{m}$  distance to the border. The dimensions of the cuboid varied from 3.3x1.7x1.7  $\mu\text{m}$  to 20x20x20  $\mu\text{m}$ .

### 3.2 Agents

The bacteria and the AI molecules are the agents of the proposed model. Table 3 shows the overall interaction rules and structural properties of the cells and the AI agent present, according to the QS mechanisms.

**Table 3.** Basic agent properties and interaction rules in the QS simulations

Agents	Structural properties	Interaction rules
AI	Radius, diffusion coefficient, and concentration	Signal sent from an organism that forms a complex with the receptor
Cell x	Shape, size	Secrets AI molecule
Cell y	Shape, size	Absorbs AI molecule

As previously mentioned, two QS systems were considered. One using peptides as their AIs and *S. mitis* and *S. mutans* as the cells absorbing and releasing the molecule, respectively. The other pertaining to an AI2 and *S. mitis* and *P. aeruginosa* as the cells releasing and absorbing the inducer, respectively. Table 4 shows the dimensions of the cells considered for both biofilms, as well as their volumes and AI molecules. Overall, the cell sizes were the same for all the simulations. For a specific simulation with *P. aeruginosa*, the length of the cell was changed in order to assess the impact of cell dimensions in the uptake of the QS molecule. R-thmf was the choice of AI2 because of the articles found, when talking about AI2 it focused more on this form instead of the others.

**Table 4.** Cells used and their autoinducer, dimensions and volume.

Cell	AI	Radius ( $\mu\text{m}$ )	Length ( $\mu\text{m}$ )	Volume ( $\mu\text{m}^3$ )
<i>Streptococcus mutans</i>	CSP	0.5	-	0.524
<i>Streptococcus mitis</i>	CSP/ r-thmf	0.8	-	2.145
<i>Pseudomonas aeruginosa</i>	r-thmf	0.5	1.5-3	1.702-2.880

The concentration, hydrodynamic radius, initial spatial location, diffusion coefficient, and movement direction are also needed for the characterization of the agents. All these topics will be addressed next.

#### 3.2.1 Concentration

The concentrations of AI molecules should be above a critical threshold, below which there are no observable effects on the cells. For AI2 molecules this threshold is between 0.8 and 1 nM (Pereira et al., 2013), for peptides, is 0.2 nM (Verbeke et al., 2017), while for AHL the concentration should be between 1 and 10 nM, the typically estimated concentration in microbial cultures (Pérez-Rodríguez et al., 2018). The number of released AIs was usually kept at 5000 molecules at the beginning of the simulation. For the biggest volume used, 20x20x20  $\mu\text{m}$ , the concentration with this number of molecules was 1.038 nM, which is above the threshold for both the peptide and the AI2.

### 3.2.2 Hydrodynamic radius

The hydrodynamic radius is the radius of a sphere that will diffuse at a similar rate to the original non-spherical molecule (Gameiro et al., 2016). A possible approximation is by the van der Waals radius (nm), which is calculated using equation 1 (Zhao et al., 2003):

$$r \text{ (nm)} = \sqrt[3]{\left(\frac{3}{4\pi}\right) \left[ \left( \sum_i^{atom} V_i \right) - 5.92N_B - 14.7R_A - 3.8R_{NA} \right]} \times 10^{-3} \quad \text{Equation 1}$$

$V_i$  corresponds to the van der Waals volume of each atom of the molecule,  $N_B$  the number of bounds,  $R_A$  the number of aromatic rings, and  $R_{NA}$  of the non-aromatic rings. The data for the van der Waals volume of each atom was obtained from Zhao et al. (2003).

For the hydrodynamic radius of proteins, the following correlation was used (Kalwarczyk et al., 2012).

$$r \text{ (nm)} = 0.0515M_w^{0.392} \quad \text{Equation 2}$$

### 3.2.3 Diffusion coefficient

Molecular diffusion is the rate of movement of each molecule on a medium and is calculated in units of area per time ( $m^2/s$ ). This coefficient can be obtained through equation 3 (the Stokes-Einstein equation), which establishes the diffusion of spheres on a liquid (Pérez-Rodríguez et al., 2018):

$$D_C(m^2/s) = \frac{k_B T}{6\pi\eta r} \quad \text{Equation 3}$$

$k_B$  is the Boltzmann's constant,  $T$  the absolute temperature,  $r$  the hydrodynamic radius, and  $\eta$  the viscosity of the medium.

The square-root law of Brownian motion was applied to implement the random walk of the molecules (Cecconi et al., 2005), as seen on Figure 6.

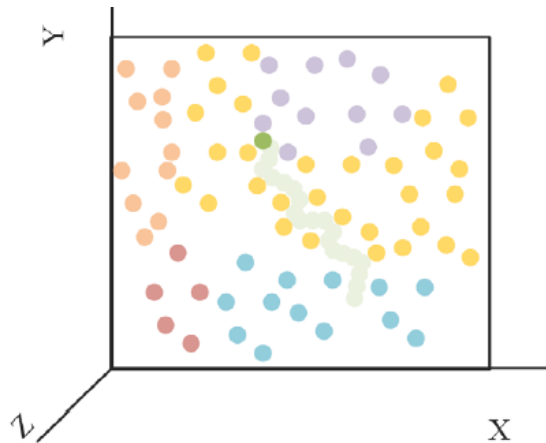


**Figure 6.** Brownian motion in a crowded environment. The movement occurs by collision with the surrounding agents. The green line shows an example of movement for the green dot. Adapted from Pérez-Rodríguez et al., 2018.

With the information previously discussed, the radius and diffusion were calculated (Table 5), with the molecular weight, hydrodynamic radius, and diffusion coefficient of the inducers.

**Table 5.** AI molecular weight, radius, and diffusion coefficient for the ABM model

Molecule	Mw (g/mol)	r (nm)	Dc (m <sup>2</sup> /s)
CSP	2242.7	1.06	2.63x10 <sup>-10</sup>
r-thmf	150.1299	0.01	2.76x10 <sup>-8</sup>

### 3.2.4 Initial spatial location and movement direction

The starting point of the agent and, if the agent moves, the direction of said movement must be defined at the start of the simulation. For the cells, only the starting point matters. Cell position was either defined (e.g. when the distance between the cells had to be defined) or random when the aim was to mimic more closely a naturally occurring biofilm. For the AIs, the starting position was defined to be on the boundary of the cell since they are produced inside the cells and only then released to the biofilm matrix. As there is a lack of data in the literature regarding the position in the cell from where the AIs are released, it was considered that they should be uniformly distributed on the membrane. The initial direction of movement of the AIs can be considered as if they are released perpendicularly to the cell surface or be defined as random. For all these simulations, the direction was considered perpendicular to the cell surface.

## 3.3 Rules

For the ABM to be the closest to real life, a set of rules should be implemented. These will dictate the interactions that happen when the agents collide with one another or with the environment. For the algorithm, this will happen when the distance between the centres of the colliding agents is less than the sum of their radius (Gameiro et al., 2016), as observable on Figure 7.

Nonetheless, a collision does not mean that a reaction occurs, most of them will only result in a movement direction change. The basic rule is that if the molecules collide with each other they will rebound. However, if a molecule collides with the environment boundary, it will leave such environment. On collision, molecules that can diffuse through the cell membrane, such as the AHL, will always be absorbed. The ones that need a membrane protein to act on the cell will recognize specific areas in the microbial surface. If they collide with such an area, they will be absorbed whereas, on any other area, they will rebound. In a perfect world, a computer would be able to compute small areas that correspond to the actual concentration of such proteins on the membrane. However, that would require immense computational power to complete the simulation within a feasible time frame. As to counter this problem, the whole area of the cell can be simulated as a receptor and, afterwards, only a portion of the number of molecules absorbed will be considered.



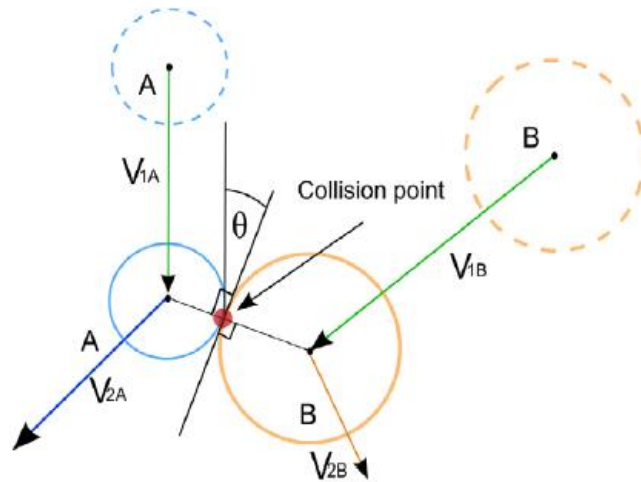


**Figure 7.** Collision detection and resolution.  $V_1$  stands for the velocity of the agents before collision, while  $V_2$  is the velocity afterwards.  $\theta$  is the deflection angle between the normal and the velocity of the agent (adapted from Pérez-Rodríguez et al., 2018).

### 3.4 Quantification of Quorum Sensing mediation

In Pérez-Rodríguez et al. (2018) a mathematical approach was developed to measure the theoretical values of the ratio of molecules that departed from the releaser cell and arrived at the receiver cell. This algebraic approach considers a realistic representation of the size and shape of the cells, as well as the perpendicular movement of AIs concerning the cell surface. In this mathematical model, no individual molecules are considered, so the correlation is obtained by calculating the surface area of one cell that, when a plane is projected perpendicularly to its surface, is capable of intersecting the other cell (Pérez-Rodríguez et al., 2018). The tests conducted on this paper were with a coccus and a bacillus cell, where they considered the bacillus aligned by an x or by a y/z axis. In other words, if it is perpendicular or parallel to the coccus, respectively, as can be seen in Figure 8.

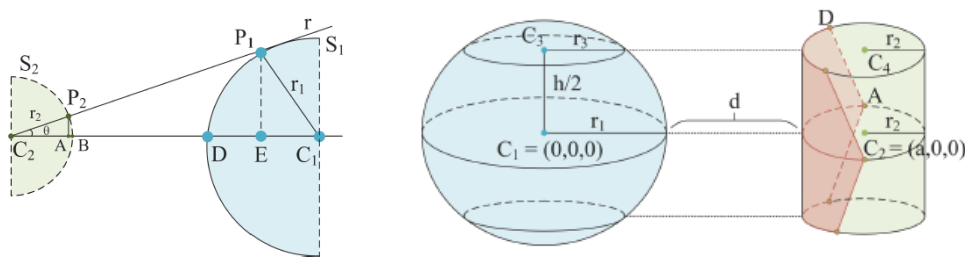


**Figure 8.** Schematic diagram of the spheric cell  $S_1$  and the spherocylinder one  $S_2$ , when they are perpendicular to each other. Only the spherical end of the bacillus was considered because that was the main part that was able to interact, through the AIs, with the coccus (left). Schematic diagram of the sphere cell and the spherocylinder one, when they are parallel to each other. Only the cylindric centre of the bacillus was considered because that was the main part that was able to interact, through the AIs, with the coccus (right).

Equation 4 estimates the ratio of the test in which the cells are perpendicular to each other.

$$\frac{A_{sup}}{A_{tot}} = \frac{r_1 r_2 (r_1 + r_2 + d - \sqrt{(r_1 + r_2 + d)^2 - r_1^2})}{(r_1 + r_2 + d)^2 (2r_2 + h)} \quad \text{Equation 4}$$

Where  $A_{sup}/A_{tot}$  represents the ratio,  $r_1$  and  $r_2$  the radii of the receptor and the releaser cell, respectively,  $h$  the height of the releaser, and  $d$  is the distance between both cells.

Since for the perpendicular cells only the spherical end was considered, the same logic can be applied for 2 cocci, where the  $A_{sup}$  is the same, changing only the total area of releaser cell to a sphere instead of the spherocylinder. This will allow obtaining the following equation.

$$\frac{A_{sup}}{A_{tot}} = \frac{r_1 (r_1 + r_2 + d - \sqrt{(r_1 + r_2 + d)^2 - r_1^2})}{2(r_1 + r_2 + d)^2} \quad \text{Equation 5}$$

### 3.5 Simulation settings

The program used was MASON, version 20, supported by Java, version 1.8.0\_291, on a computer with an AMD Phenom(tm) II X4 965 Processor, 3400 Mhz and 8 Gb of RAM DDR3 @ 669.6 Mhz CL9 running Windows 7 Ultimate 64 bits.

### 3.6 Simulations

Initially, the influence of the distance between the two cells in the uptake of QS molecules was tested for the pairs of cells *S. mutans* - *S. mitis* and *S. mitis* - *P. aeruginosa*. This test allowed the validation of the simulation against the previously referred mathematical model. Distances of 0.1  $\mu\text{m}$  and between 0.5 and 10  $\mu\text{m}$ , with intervals of 0.5  $\mu\text{m}$  were tested, where the orientation was also analysed for the spherocylinder, *P. aeruginosa*, testing it when they were horizontally aligned, that is aligned by an imaginary x-axis, as seen in Figure 9. Using distances of 5  $\mu\text{m}$ , the influence of the size of the receptor cell was also tested on the duo *S. mitis* and *P. aeruginosa*, where the length of the later varied between 1.5, 2, 2.5 and 3  $\mu\text{m}$ .

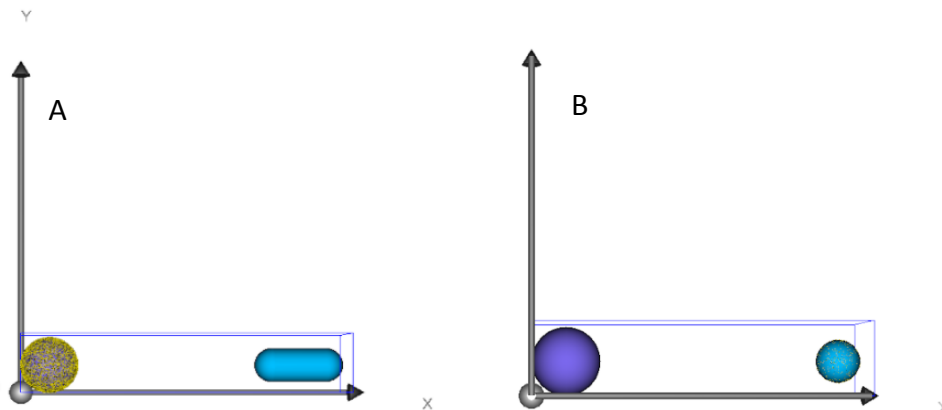


**Figure 9.** Example of the position of the cells on tests between *S. mitis* and *P. aeruginosa*, when they are aligned horizontally (A), and *S. mitis* and *S. mutans* (B), both at 5  $\mu\text{m}$ .

The cells, when on the biofilm, do not just communicate with the cell that is right on their side, so tests with inducers provided from the environment borders were also done for both pairs of cells. The length of the *P. aeruginosa* was kept at 1.5  $\mu\text{m}$  for the test and the number of AIs released by the environment was 600 new molecules every 10000 steps. This allows the maintenance of a reasonable concentration of AIs for the duration of the experiment, so the concentration of molecules would be way too high when compared to the minimum threshold. A representation of the simulation is in Figure 10-A.

The fourth group of tests consists of both cells releasing AIs (Figure 10-B). This was tested because, in a biofilm, all cells release molecules to the surrounding environment. Both pairs of cells were tested. However, as previously mentioned the *P. aeruginosa* cannot produce the AI2 that is being tested, so an AHL was chosen to be released by *P. aeruginosa* since they can produce this type of AI. The release of the AI from the cell that was, previously, only the receptor, was the same as the defined for the releaser cell, 5000 AIs at the beginning of the simulation.

The final group of tests was done considering 4 *S. mitis* on randomized positions on the environment to see how the concentration on the medium evolved with time (Figure 10-C). Each cell released 50 AIs every 10000 steps.

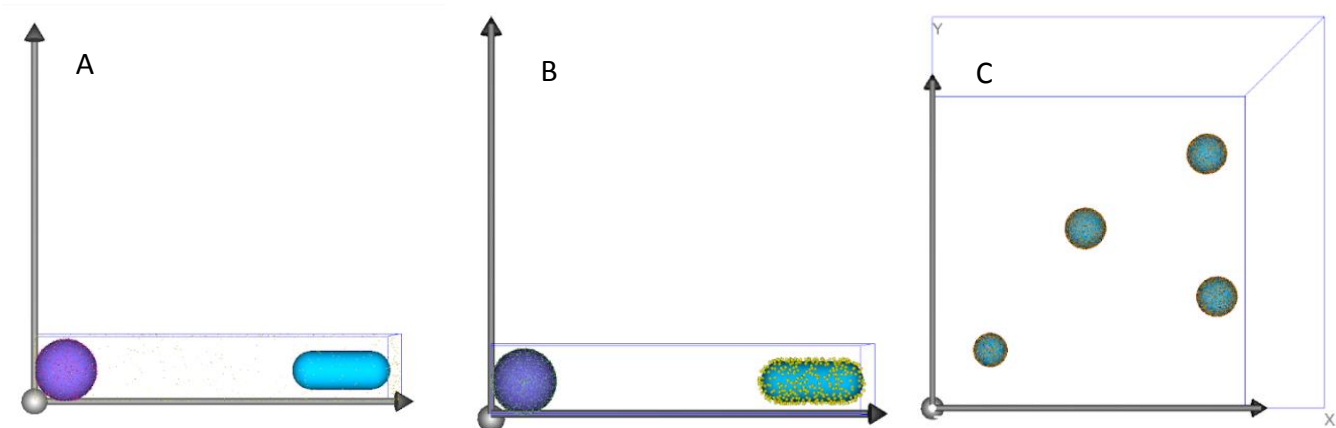


**Figure 10.** Example of the environment feeding test between *S. mitis* and *P. aeruginosa*, when they are aligned horizontally, at 5  $\mu\text{m}$  (A). Example of the dual feeding test between *S. mitis* and *P. aeruginosa*, when they are aligned horizontally, at 5  $\mu\text{m}$  (B). Example of the test between several *S. mitis* positioned randomly (C).

### 3.7 Statistical Analysis

Five replicates were made for each computational simulation. The results of these tests were compared between each other using the Wilcoxon matching pairs test and between the mathematical model with the one-sample Wilcoxon test, non-parametric alternatives to the t-test, since the size of the population was small, and they do not require the data to follow a normal distribution (analysed through a QQ plot). The significance level was kept at 5% ( $p < 0.05$ ).

## 4 Results and discussion

Before the tests started, a validation of the distribution of the molecules released from the cell surface of *S. mitis* and *P. aeruginosa* was performed. These microorganisms represent the two cell morphologies used in this thesis, coccoid and rod-shaped (Iglewski, 1996; Ryan & Ray, 2003). According to the literature, the secretion of the AI2 and the AHL is through passive diffusion on the cell membrane (Vendeville et al., 2005; Waters & Bassler, 2005), and as such an approximately equal distribution across the cell membrane is expected. Even though it is known that the peptides are released via active diffusion (Salvadori et al., 2018), there isn't any indication that the membrane protein isn't equally distributed on the cell membrane. The results obtained for the distribution of AIs in the surface of *S. mitis* and *P. aeruginosa* indicate that the distribution was, approximately, equal on all octants of the releaser cell, which gives validation on the assumption that the distribution was uniform on the cell membrane (Figure 11). It is important to bear in mind that if it was experimentally determined that the inducers are secreted through a preferable zone of the cell, the simulation can be easily adjustable.

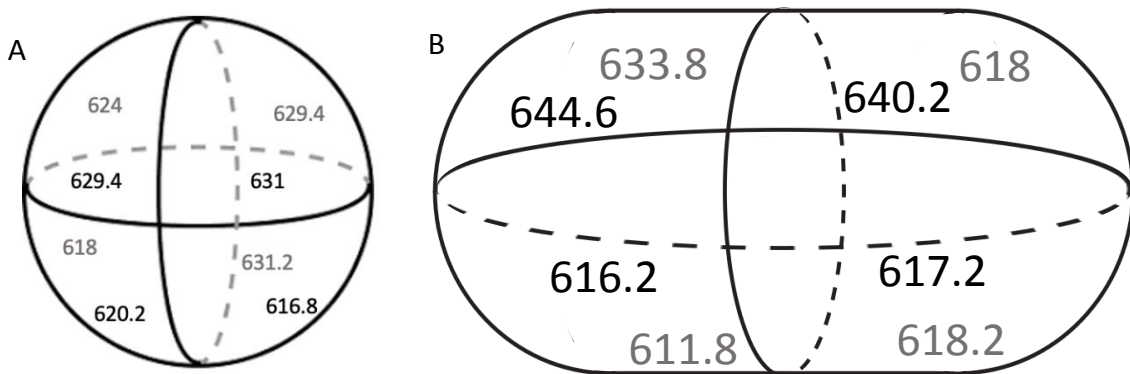


**Figure 11.** Distribution of AIs on the different octants of the releaser cells of each shape (*S. mitis* – A; *P. aeruginosa* – B). The grey numbers represent the number of AIs released on the back octants, while the black represents the ones released on the front octants.

A second validation assessed the influence of the distance on AI uptake, underlining the importance of the distance over the communication with AIs between cells in comparison to the mathematical model that was previously described (Pérez-Rodríguez et al., 2018). These graphs were subdivided on multiple graphs, each with three distances, so more detail on every value of the different distances are presented in the Annexes.

For groups 1 (pair *S. mitis* and *P. aeruginosa* aligned horizontally) and 2 (pair *S. mitis* and *S. mutans*) (Figure 12) the distances negatively affected the fraction of the AIs that collided with the target cell. With larger distances, it was also observed that the difference in values of absorbed AIs was not considered statistically significant. Comparing to each other, overall, group 2 has a higher percentage of absorbed AIs. The explanation lies on the size of the inducers (the peptides are larger so there is a higher change

they collide with the receptor) and on the size of the receptor (the sphere is larger than the spherical side of the spherocylinder).

When compared to the mathematical model values, in general, the simulation had higher percentages of absorbed AIs, being those differences statistically significant. For group 1 the largest difference was 0.98 % when the distance was 0.1  $\mu\text{m}$ , and for group 2 the difference was 1.10 %, when the distance was 0.5  $\mu\text{m}$ . These differences can be explained by a number of reasons. Firstly, molecular collisions are random, and their influence can significantly alter the values in comparison to the mathematical model, that does not contemplate it. Specially at greater distances, where the expected uptake of the number of AIs was so low that the difference between them would significantly alter the uptake of only 1 AI. The mathematical model considers as well that the size of the molecules is infinitesimally small, instead of considering their real dimension (Pérez-Rodríguez et al., 2018).

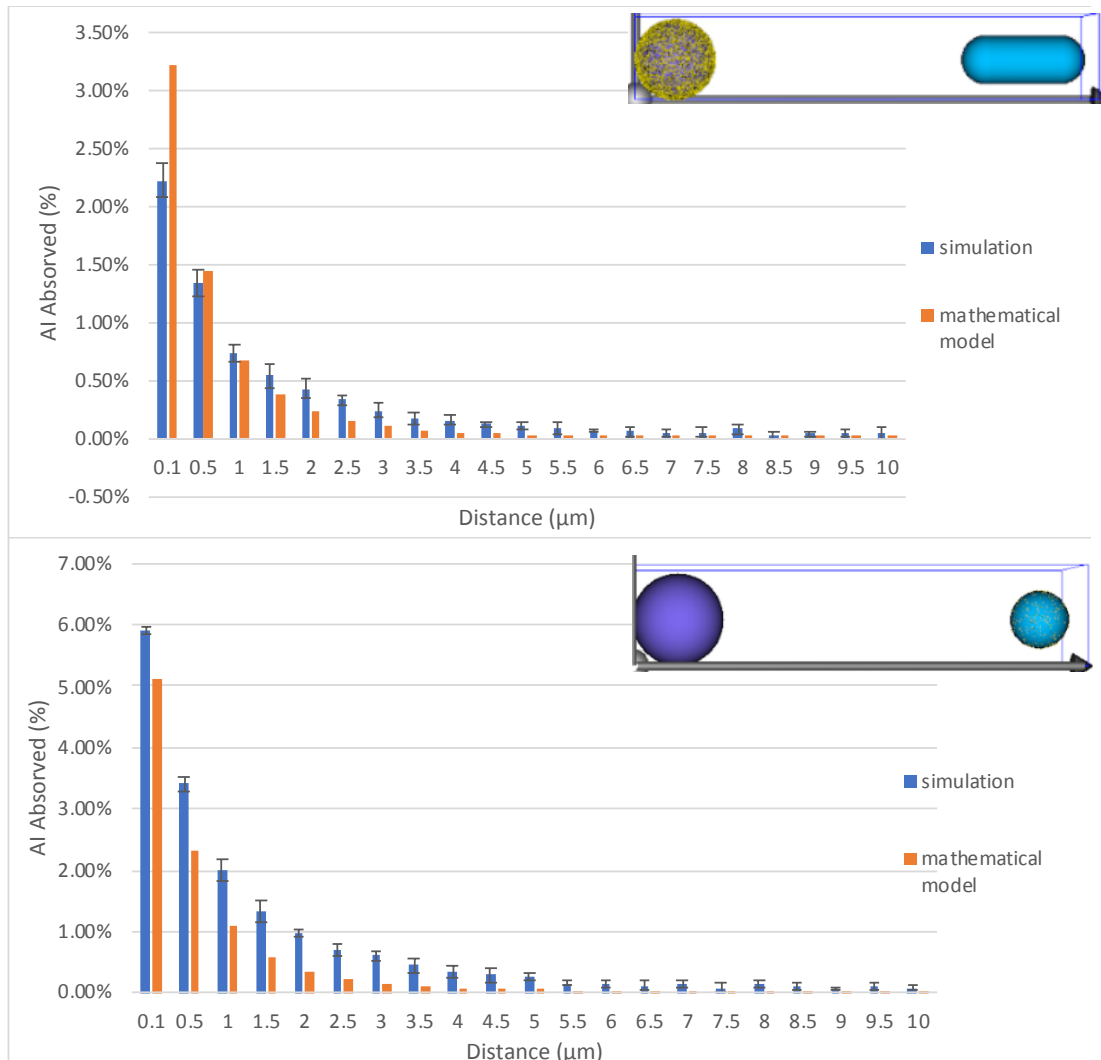


**Figure 12.** Results for the algebraic approach and simulation tests of *P. aeruginosa* and *S. mitis* (above) *S. mutans* and *S. mitis* (below) at different distances, where the former of each duo is the one releasing the sensor molecule.

A final validation was the mean time it took for the cell to uptake the AI. As expected, the greater the distances the greater the time the uptake took, following a linear correlation (Figure 13). This also gives

validation to the simulation. Since the diffusion is expected to be the same on all tests, it is anticipated that a linear correlation is followed when comparing the time that occurred to reach one cell from the other at different distances.

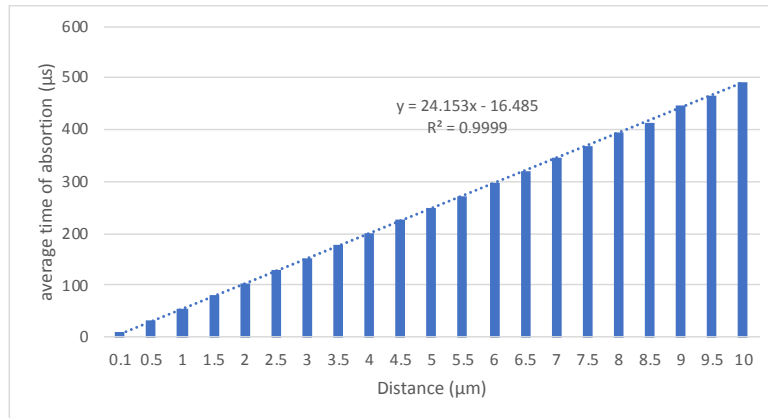


**Figure 13.** Average time a molecule took to be absorbed by the receptor cell for each of the distances tested, for the duo *S. mitis* and *P. aeruginosa*, aligned horizontally.

After these validations, tests were performed with *P. aeruginosa* aligned vertically when compared to *S. mitis*, i.e., aligned by an imaginary y-axis (group 3) (Figure 14). This alignment will make a cylinder face *S. mitis*, instead of the sphere that was represented on previous tests. For this situation, there is no



**Figure 14.** Example of the position of the cells on a test between *S. mitis* and *P. aeruginosa*, when they are aligned vertically, at 5 µm.

mathematical model described in the literature.

These graphs were subdivided on multiple graphs with three distances so more detail on every value of the different distances can be analysed. They are present in the Annex. As observable in figure 15, an increase in the distance is unfavourable for AI uptake on the receptor cell and, at greater distances, the different percentages started to be considered not statistically significant. These results are, as expected, similar to the ones found in groups 1 and 2. When compared to group 1, the percentages are clearly

higher. This happens because, on this test, the part facing the releaser cell is a cylinder, which as a larger surface area than the spherical part facing previously (the sphere as a 0.5 μm radius, while the cylinder as the same radius and a length of 1.5 μm).

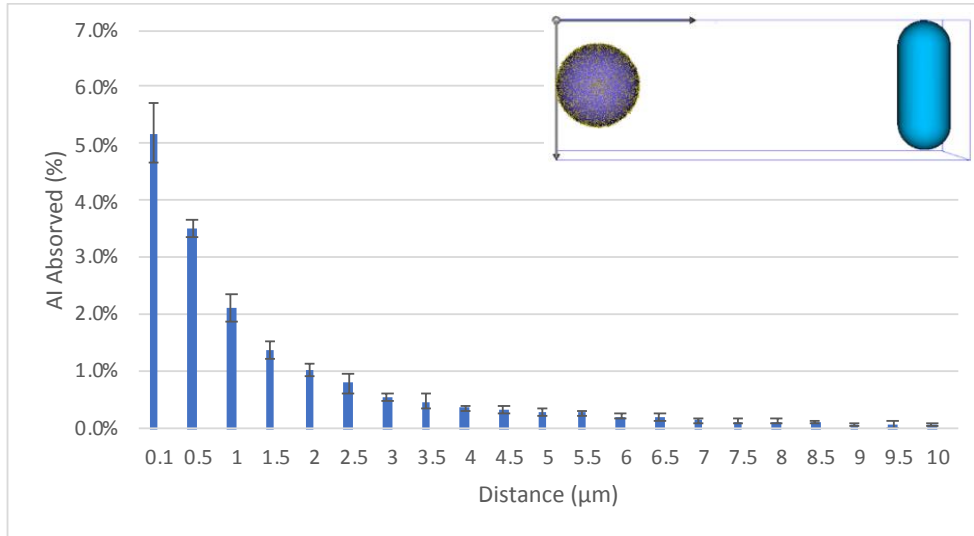


**Figure 15.** Results for the simulation tests of *S. mitis* and *P. aeruginosa* aligned vertically at different distances, where the former is the one releasing the sensor molecule

The next group of tests focused on the length of the spherocylinder as the receptor. The results for groups 1 and 3 are grouped in Figure 16. As referred above, *P. aeruginosa* usually has cell lengths that varies between 1.5 and 3 μm (Iglewski, 1996). However, there are some mutants that can achieve lengths of 10 μm. Still, these cells are more susceptible to antibiotics, which prevents them from division (Deforet et al., 2015).

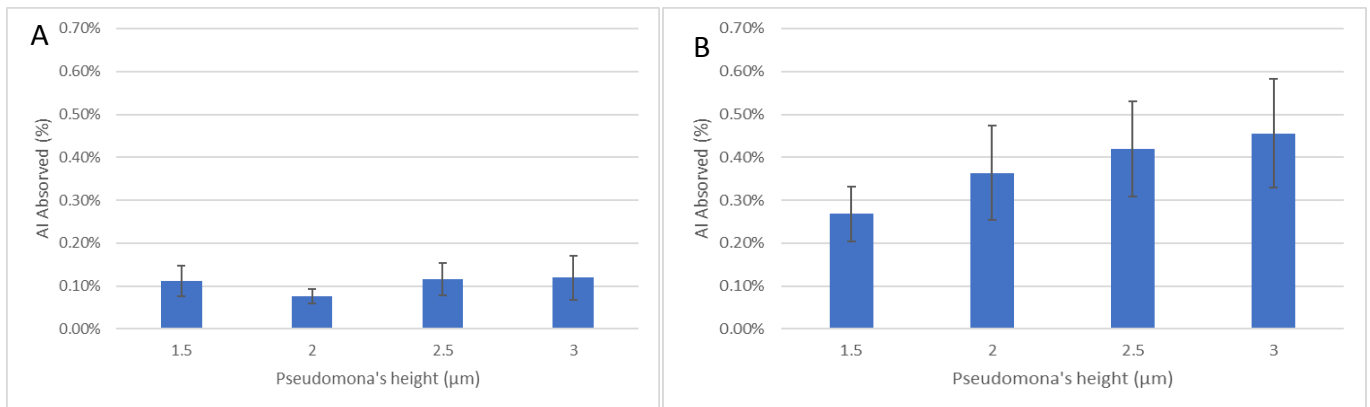


**Figure 16.** Results for the simulation tests of *S. mitis* and *P. aeruginosa* aligned horizontally (A) and vertically (B) for different length values of the *P. aeruginosa*, where the former is the one releasing the sensor molecule.

For group 1 (Figure 16 – A), when a sphere is facing *S. mitis* it was expected that no change would occur, since only the cylinder part suffered changes. In group 3 (Figure 16 – B) some differences are expected since the cylinder is now the one facing the releaser cell and with a longer cell, the higher the chances that the AI will collide with the cell. In both cases, the differences in percentages of absorbed AIs are not

statistically significant. The biggest difference found was between lengths 1.5 and 3  $\mu\text{m}$ , 0.19%, on group 3. The change englobed a few lengths, from the smallest to the biggest possible, according to the literature, and the results showed that this difference in these sizes of the receptor cell does not seem to affect the communication between the cells. Even if it is not statistically significant, it is noticeable a small growth on the uptake of AIs between cell lengths on group 3. Which might mean that if the mutants previously mentioned reach larger lengths these differences might be significant, and the cells have a better uptake of the inducers.

Tests with inducers released from the boundaries of the environment simultaneously with the release from the cells were also done. This environmental feeding can be an aspect that might significantly affect the communication between two cells and was simulated to represent the inducers released from cells that are outside the boundaries of the simulation volume. The results are showcased in Figure 17.

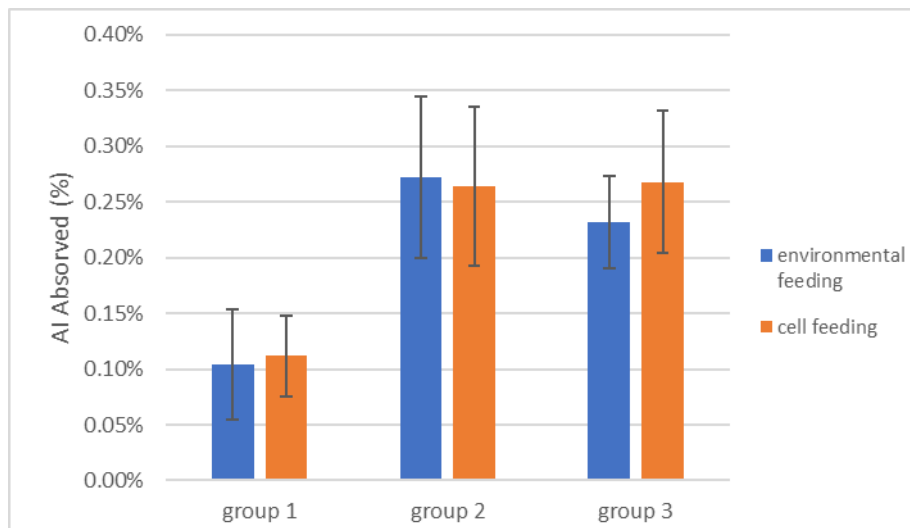


**Figure 17.** Results of the simulations tests of an additional environmental feeding compared to feeding from only a single cell.

When compared to the tests with no extra feeding, the results did not change much, the differences are not statistically significant, being the biggest difference on group 3, 0.036%. These results indicate that environmental feeding does not affect the feeding from one cell to another.

Dual cell feeding was introduced in the following simulations. The dual feeding showed the same conclusions as the environmental feeding with changes statistically insignificant to the values of the molecules that were uptake (Figure 18), the biggest difference was found in group 1, 0.028 %. So, the same conclusion can be taken, the simultaneous feeding on both cells does not seem to affect the feeding and the percentage of absorbed molecules as if only 1 of the cells was producing AIs.



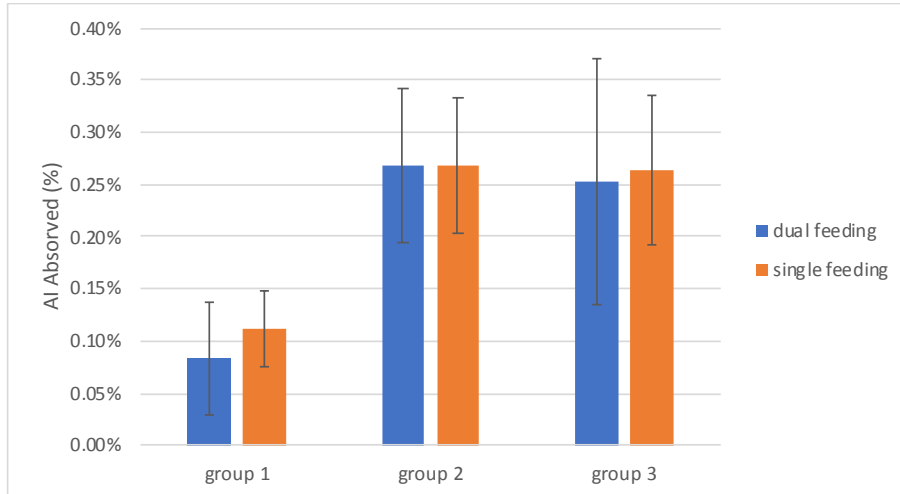


Figure 18. Results of the simulations tests of feeding from both cells compared to feeding from a single cell.

The last group of simulations consisted of four *S. mitis* all releasing AIs over time to the environment, in order to analyse the variation of concentration over time. The results are shown in Figure 19.

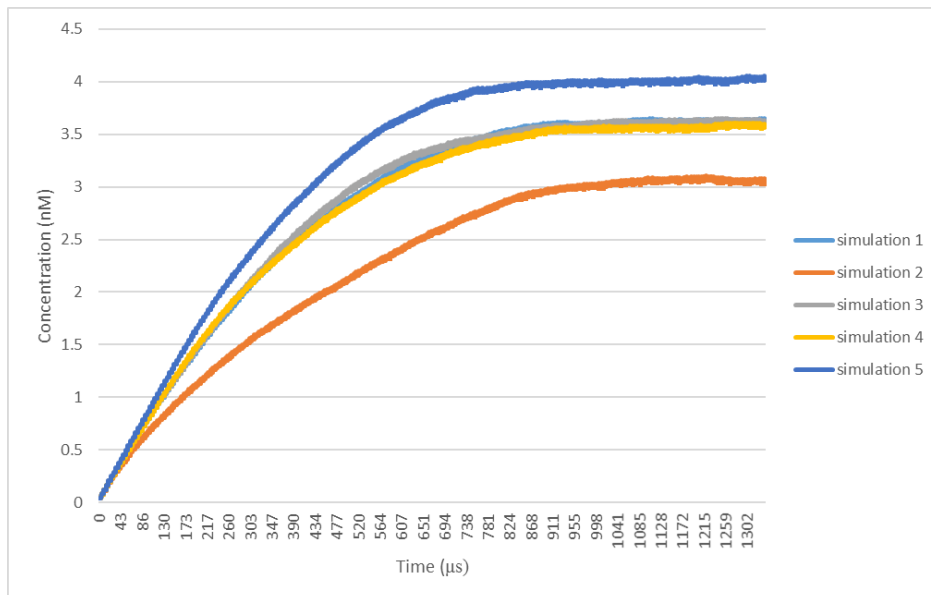


Figure 19. Results of the simulations with four *S. mitis* randomly positioned.

It is observable that in all 5 simulations a steady state was achieved, where the number of AIs released by the cells were sensibly the same as the molecules leaving the environment and being absorbed by the other cells. This was achieved between, approximately, 750 and 900  $\mu\text{s}$ . The difference in these times and the concentration achieved can be explained by the random position in which the cells are allocated in each simulation.

The assumptions made eased the construction of the model, while maintaining it as realistic as possible. However, some adjustments were made in order to ease the construction of the model and due to the lack of some biological data. The viscosity of the medium can be considered the same as water at 30 °C because this is a good temperature for biofilm formation (Else et al., 2003) and the concentration of other molecules is small (biofilms are composed by 70-95% of water, the rest being the molecules present on

the cell, like the membrane and the EPS (H. C. Flemming, 1993)). Other molecules, that may be present on the extracellular medium, were not considered, due to their small concentration on the medium and to not overcrowd the environment, making the simulation run slower. For the AI, a spherical approximation is a typical effective way to create a realistic and computer tractable representation of molecules (Feig & Sugita, 2013). It was also considered that they can easily diffuse through the membrane and are detected inside the cell, even though for both QS tested the AI is absorbed via a membrane receptor. However, there is not enough information about the receptors to assume any values about their distribution on the membrane. Only two types of cells were contemplated for each biofilm, even though there may be more present, since the logic applied to these pairs of cells can also be applied to other cells of the same shape. Which would make redundant the use of more species of the same shape, more cells represented would also overcrowd the environment. The consideration of non-motile cells is also realistic because they are inside a biofilm and encased in a matrix and their size was considered constant during time since the time intervals are so low that change in size can be considered irrelevant. The behaviour of the agents was considered the same on every section of the biofilm, so a representation of a small section of the biofilm could represent, approximately, the behaviour of the agents on the whole biofilm. This last assumption is needed due to the impossibility of representing a full biofilm, which implies the use of many individual cells and plenty of different molecules. This is not possible on the average computers used on these simulations. Extra biological data would be a great advantage and would help to create an even more realistic environment for the study of these biofilms. However, with the information that was available and found at the time of this work a more realistic approach was still possible, when compared to the approaches made to date.

Most models applied to this day on biofilms, from stochastic individual-based models (Hong et al., 2007), to deterministic differential equation models (Schroeder et al., 2015) and even hybrid models (Weber & Buceta, 2013), share one thing in common: complexity, which is a major hindrance. Even though these models provide the most detailed and realistic representation, their complexity prevents further exploration of the full dynamic (Pérez-Velázquez et al., 2016). The dominant advantage of ABM is the reduction of complexity in the model. In particular, ABM can supply detailed information about complex scenarios, including multiple cells on a random distribution, and simulate multiple scenarios of spatial distribution, involving different kinds of feeding. ABM does multiple types of tests while keeping a simple model with the need to only describe the environment, agents and the rules of their behaviour.

## 5 Conclusions

The present work focused on the application of ABMs and potential to understand quorum sensing communication in biofilms. ABMs allowed to study of the impact of several factors, including cell location, orientation and the existence/absence of feeding from the environment. For the first time, ABM was applied to peptide and AI2 QS systems, instead of the most well-studied, AHL. It also analysed a new type of feeding on ABM, the dual feeding where both cells released inducers. This study also highlighted the ease of working with this type of model and the usefulness it can provide on these types of studies.

The comparison between the ABMs and the mathematical model showed a maximum difference of 1.1 % in AI uptake, meaning that the ABM provides realistic results for the simplest situations where mathematical equations can still be obtained. The small differences obtained can be explained by two main causes: the physical dimensions of the AIs and molecular collisions, with the implied change in trajectory.

The study of different types of feeding showed that the uptake of the inducers released from one cell does not seem to be affected by the presence of other feeding systems, namely environmental feeding and from both cells. The length of the cells did not seem to affect the uptake of AIs, with differences not statistically significant between the different lengths. However, a small increase in the percentage of AI uptake is noticed when the spherocylinder is vertically aligned to the releaser cell. This means that if a cell are longer, the differences might be significant, which means that the uptake is higher with longer cells.

## 6 Limitations and Future Work

The biggest limitation to this work is the lack of biological data for some aspects. For example, even though it is known that the AIs tested are all absorbed by membrane receptors, there is not enough information about them, namely how many are present in the membrane and how they are distributed. Having more data would contribute to the reduction of the assumptions made. Other limitations were the computers not being able to process environments that are overcrowded, taking a long time to finish the desired tests and that limited our simulations to a maximum number of approximately 12000 agents. In the future, as computers and methods of tracking evolve and more information is made available, it would be interesting to try to simulate the internal signalling of the receptor cells after receiving the inducer, until the creation and release to the environment of more inducers, which would then be absorbed by other cells. Regarding simulation performance, high performance strategies will be investigated. While three dimensional simulators are still uncommon, previous work on applying concurrent and distributed computing in ABM simulation are a good basis to develop better equipped simulators (Pérez-Rodríguez et al., 2016, 2018). Additional complexity could also be added to the model; for example, the uptake of a specific AI could lead to cell replication or detachment of cells from the biofilm (Emerenini et al., 2015). The first example would help understanding, for instance, the growth of the biofilm by the means of reproduction of the cells already present in the biofilm. It would also be interesting to test a hundred or more cells to simulate a larger volume of the biofilm environment. Tests with multiple QS systems present, with different molecules of the same group present would be interesting, with different cells detecting different molecules. The experiments would reproduce multiple QS systems, including species that have QS systems releasing different molecules, and other species relying only in one system.

## References

- Antunes, L. C. M., Ferreira, R. B. R., Buckner, M. M. C., & Finlay, B. B. (2010). Quorum sensing in bacterial virulence. *Microbiology*, *156*(8), 2271–2282. <https://doi.org/10.1099/mic.0.038794-0>
- ASAE homepage. (n.d.). Retrieved November 10, 2020, from <https://www.asae.gov.pt/>
- Balzer, M., Witt, N., Flemming, H.-C., & Wingender, J. (2010). Accumulation of Fecal Indicator Bacteria in River. *Water Science and Technology*, *61*, 1105–1110.
- Biebl, H., Allgaier, M., Tindall, B. J., Koblizek, M., Lünsdorf, H., Pukall, R., & Wagner-Döbler, I. (2005). *Dinoroseobacter shibae* gen. nov., sp. nov., a new aerobic phototrophic bacterium isolated from dinoflagellates. *International Journal of Systematic and Evolutionary Microbiology*, *55*(3), 1089–1096. <https://doi.org/10.1099/ijs.0.63511-0>
- Bikash, C. R., Hamry, S. R., & Tal-Gan, Y. (2018). Structure-Activity Relationships of the Competence Stimulating Peptide in *Streptococcus mutans* Reveal Motifs Critical for Membrane Protease SepM Recognition and ComD Receptor Activation. *ACS Infectious Diseases*, *4*(9), 1385–1394. <https://doi.org/10.1021/acsinfecdis.8b00115>
- Bikash, C. R., & Tal-Gan, Y. (2019). Identification of highly potent competence stimulating peptide-based quorum sensing activators in *Streptococcus mutans* through the utilization of N-methyl and reverse alanine scanning. *Bioorganic and Medicinal Chemistry Letters*, *29*(6), 811–814. <https://doi.org/10.1016/j.bmcl.2019.01.029>
- Bodine, E. N., Panoff, R. M., Voit, E. O., & Weisstein, A. E. (2020). Agent-Based Modeling and Simulation in Mathematics and Biology Education. *Bulletin of Mathematical Biology*, *82*(8). <https://doi.org/10.1007/s11538-020-00778-z>
- Bonabeau, E. (2002). Agent-based modelling: Methods and techniques for simulating human systems. *Proceedings of the National Academy of Sciences of the United States of America*, *99*(3), 7280–7287.
- Borges, A., & Simões, M. (2019). Quorum sensing inhibition by marine bacteria. *Marine Drugs*, *17*(7). <https://doi.org/10.3390/md17070427>
- Britannica homepage. (n.d.). Retrieved November 10, 2020, from <https://www.britannica.com/>
- Caruso, F. L., & Ramsdell, D. C. (2014). Compendium of Blueberry and Cranberry Diseases. *Journal of Plant Pathology*, *96*(2), 431–439.
- Castiglione, F. (2009). Introduction to agent-based modeling and simulation. In *Encyclopedia of Complexity and Systems Science*. (1st ed., pp. 197–200).
- CDC homepage. (n.d.). Retrieved November 10, 2020, from <https://www.cdc.gov/>
- Cecconi, F., Cencini, M., Falcioni, M., & Vulpiani, A. (2005). Brownian motion and diffusion: From

- stochastic processes to chaos and beyond. *Chaos*, 15(2). <https://doi.org/10.1063/1.1832773>
- Chen, L., Wilksch, J. J., Liu, H., Zhang, X., Torres, V. V. L., Bi, W., Mandela, E., Cao, J., Li, J., Lithgow, T., & Zhou, T. (2020). Investigation of LuxS-mediated quorum sensing in *Klebsiella pneumoniae*. *JOURNAL OF MEDICAL MICROBIOLOGY*, 69(3), 402–413.
- Cheng, J., Sibley, C. D., Zaheer, R., & Finan, T. M. (2007). A *Sinorhizobium meliloti* minE mutant has an altered morphology and exhibits defects in legume symbiosis. *Microbiology*, 153(2), 375–387. <https://doi.org/10.1099/mic.0.2006/001362-0>
- Christen, M., & Van Gunsteren, W. F. (2006). Multigraining: An algorithm for simultaneous fine-grained and coarse-grained simulation of molecular systems. *Journal of Chemical Physics*, 124(15). <https://doi.org/10.1063/1.2187488>
- Costerton, J. W., Cheng, K. J., Geesey, G. G., Ladd, T. I., Nickel, J. C., Dasgupta, M., & Marrie, T. J. (1987). Bacterial biofilms in nature and disease. *Annual Review of Microbiology*, 41, 435–464. <https://doi.org/10.1146/annurev.mi.41.100187.002251>
- Crooks, A. T., & Heppenstall, A. J. (2012). Introduction to agent-based modelling. In *Agent-Based Models of Geographical Systems* (pp. 85–105). [https://doi.org/10.1007/978-90-481-8927-4\\_5](https://doi.org/10.1007/978-90-481-8927-4_5)
- Cruz, R. L., Asfahl, K. L., Van den Bossche, S., Coenye, T., Crabbé, A., & Dandekar, A. A. (2020). RhlR-regulated acyl-homoserine lactone quorum sensing in a cystic fibrosis isolate of *Pseudomonas aeruginosa*. *MBio*, 11(2). <https://doi.org/10.1128/mBio.00532-20>
- Davidsson, P., Holmgren, J., Kyhlbäck, H., Mengistu, D., & Persson, M. (2007). Applications of agent based simulation. *Lecture Notes in Computer Science (Including Subseries Lecture Notes in Artificial Intelligence and Lecture Notes in Bioinformatics)*, 4442 LNAI, 15–27. [https://doi.org/10.1007/978-3-540-76539-4\\_2](https://doi.org/10.1007/978-3-540-76539-4_2)
- Davies, D. G., Parsek, M. R., Pearson, J. P., Iglewski, B. H., Costerton, J. W., & Greenberg, J. W. (1998). The involvement of cell-to-cell signals in the development of a bacterial biofilm. *Science*, 280, 295–298.
- De Kievit, T. R. (2009). Quorum sensing in *Pseudomonas aeruginosa* biofilms. *Environmental Microbiology*, 11(2), 279–288. <https://doi.org/10.1111/j.1462-2920.2008.01792.x>
- Deforet, M., Van Ditmarsch, D., & Xavier, J. B. (2015). Cell-Size Homeostasis and the Incremental Rule in a Bacterial Pathogen. *Biophysical Journal*, 109(3), 521–528. <https://doi.org/10.1016/j.bpj.2015.07.002>
- Donlan, R. M. (2001). Biofilm formation: A clinically relevant microbiological process. In *Clinical Infectious Diseases* (Vol. 33, Issue 8, pp. 1387–1392). <https://doi.org/10.1086/322972>
- Else, T. A., Pantle, C. R., & Amy, P. S. (2003). Boundaries for biofilm formation: Humidity and temperature. *Applied and Environmental Microbiology*, 69(8), 5006–5010.

- <https://doi.org/10.1128/AEM.69.8.5006-5010.2003>
- Embers, M. E., Doyle, L. A., Whitehouse, C. A., Selby, E. B., Chappell, M., & Philipp, M. T. (2011). Characterization of a *Moraxella* species that causes epistaxis in macaques. *Veterinary Microbiology*, *147*(3–4), 367–375. <https://doi.org/10.1016/j.vetmic.2010.06.029>
- Emerenini, B. O., Hense, B. A., Kuttler, C., & Eberl, H. J. (2015). A mathematical model of quorum sensing induced biofilm detachment. *PLoS ONE*, *10*(7). <https://doi.org/10.1371/journal.pone.0132385>
- Engbrecht, J. A., & Silverman, M. (1984). Identification of genes and gene products necessary for bacterial bioluminescence. *Proceedings of the National Academy of Sciences of the United States of America*, *81*(13), 4154–4158. <https://doi.org/10.1073/pnas.81.13.4154>
- Engbrecht, J., Neelson, K., & Silverman, M. (1983). Bacterial bioluminescence: Isolation and genetic analysis of functions from *Vibrio fischeri*. *Cell*, *32*(3), 773–781. [https://doi.org/10.1016/0092-8674\(83\)90063-6](https://doi.org/10.1016/0092-8674(83)90063-6)
- Engbrecht, J., & Silverman, M. (1987). Nucleotide sequence of the regulatory locus controlling expression of bacterial genes for bioluminescence. *Nucleic Acids Research*, *15*(24), 10455–10467. <https://doi.org/10.1093/nar/15.24.10455>
- Epstein, J. M., & Axtell, R. (1997). Growing artificial societies: Social science from the bottom up. In *Computers & Mathematics with Applications* (Vol. 33, Issue 5). [https://doi.org/10.1016/s0898-1221\(97\)82923-9](https://doi.org/10.1016/s0898-1221(97)82923-9)
- Ethelberg, S., Mølbak, K., & Josefsen, M. H. (2014). Bacteria: Salmonella Non-Typhi. *Encyclopedia of Food Safety*, *1*, 501–514. <https://doi.org/10.1016/B978-0-12-378612-8.00112-8>
- Feig, M., & Sugita, Y. (2013). Reaching new levels of realism in modeling biological macromolecules in cellular environments. *Journal of Molecular Graphics and Modelling*, *45*, 144–156. <https://doi.org/10.1016/j.jmgm.2013.08.017>
- Fekete, A., Kuttler, C., Rothballer, M., Hense, B. A., Fischer, D., Buddrus-Schiemann, K., Lucio, M., Müller, J., Schmitt-Kopplin, P., & Hartmann, A. (2010). Dynamic regulation of N-acyl-homoserine lactone production and degradation in *Pseudomonas putida* IsoF. *FEMS Microbiology Ecology*, *72*(1), 22–34. <https://doi.org/10.1111/j.1574-6941.2009.00828.x>
- Fleming, H.-C., Wingender, J., & Szewzyk, U. (2011). *Biofilm Highlights*.
- Fleming, H. C. (1993). Biofilms and environmental protection. *Water Science and Technology*, *27*(7–8), 1–10. <https://doi.org/10.2166/wst.1993.0528>
- Fleming, Hans Curt, & Wingender, J. (2010). The biofilm matrix. *Nature Reviews Microbiology*, *8*(9), 623–633. <https://doi.org/10.1038/nrmicro2415>
- Fleming, Hans Curt, Wingender, J., Szewzyk, U., Steinberg, P., Rice, S. A., & Kjelleberg, S. (2016).

- Biofilms: An emergent form of bacterial life. *Nature Reviews Microbiology*, 14(9), 563–575.  
<https://doi.org/10.1038/nrmicro.2016.94>
- Franklin, S., & Graesser, A. (1996). Is it an agent, or just a program?: A taxonomy for autonomous agent. In *Proceedings of the Third International Workshop on Agent Theories, Architectures, and Languages* (pp. 21–35).
- Gameiro, D., Pérez-Pérez, M., Pérez-Rodríguez, G., Monteiro, G., Azevedo, N. F., & Lourenço, A. (2016). Computational resources and strategies to construct single-molecule metabolic models of microbial cells. *Briefings in Bioinformatics*, 17(5), 863–876.  
<https://doi.org/10.1093/bib/bbv096>
- Ganesh, P. S., & Rai, V. R. (2018). Alternative strategies to regulate quorum sensing and biofilm formation of pathogenic pseudomonas by quorum sensing inhibitors of diverse origins. *Biotechnological Applications of Quorum Sensing Inhibitors*, 33–61.  
[https://doi.org/10.1007/978-981-10-9026-4\\_3](https://doi.org/10.1007/978-981-10-9026-4_3)
- Garrity, G. M., Bell, J. A., & Lilburn, T. (2005). The Proteobacteria. In *Bergey's Manual® of Systematic Bacteriology* (2nd ed., pp. 323–442).
- Gilbert, N., & Terna, P. (2000). How to build and use agent-based models in social science. *Mind & Society*, 1(1), 57–72. <https://doi.org/10.1007/bf02512229>
- Halan, B., Buehler, K., & Schmid, A. (2012). Biofilms as living catalysts in continuous chemical syntheses. *Trends in Biotechnology*, 30(9), 453–465.  
<https://doi.org/10.1016/j.tibtech.2012.05.003>
- Harris, L. G., Foster, S. J., Richards, R. G., Lambert, P., Stickler, D., & Eley, A. (2002). An introduction to Staphylococcus aureus, and techniques for identifying and quantifying S. aureus adhesins in relation to adhesion to biomaterials: Review. *European Cells and Materials*, 4, 39–60.  
<https://doi.org/10.22203/ecm.v004a04>
- Hong, D., Saidel, W. M., Man, S., & Martin, J. V. (2007). Extracellular noise-induced stochastic synchronization in heterogeneous quorum sensing network. *Journal of Theoretical Biology*, 245(4), 726–736. <https://doi.org/10.1016/j.jtbi.2006.12.006>
- Horneman, A. J., Ali, A., & Abbott, S. L. (2007). Aeromonas. In *Manual of Clinical Microbiology* (pp. 716–722).
- Huber, B., Riedel, K., Hentzer, M., Heydorn, A., Gotschlich, A., Givskov, M., Molin, S., & Eberl, L. (2001). The cep quorum-sensing system of Burkholderia cepacia H111 controls biofilm formation and swarming motility. *Microbiology*, 147(9), 2517–2528.  
<https://doi.org/10.1099/00221287-147-9-2517>
- Huber, Birgit, Riedel, K., Köthe, M., Givskov, M., Molin, S., & Eberl, L. (2002). Genetic analysis of



- functions involved in the late stages of biofilm development in *Burkholderia cepacia* H111. *Molecular Microbiology*, 46(2), 411–426. <https://doi.org/10.1046/j.1365-2958.2002.03182.x>
- Hultqvist, L. D., Alhede, M., Jakobsen, T. H., Givskov, M., & Bjarnsholt, T. (2018). Imaging N-acyl homoserine lactone quorum sensing in vivo. *Methods in Molecular Biology*, 1673, 203–212. [https://doi.org/10.1007/978-1-4939-7309-5\\_16](https://doi.org/10.1007/978-1-4939-7309-5_16)
- Hwang, G., Park, S. R., Lee, C. H., Ahn, I. S., Yoon, Y. J., & Mhin, B. J. (2009). Influence of naphthalene biodegradation on the adhesion of *Pseudomonas putida* NCIB 9816-4 to a naphthalene-contaminated soil. *Journal of Hazardous Materials*, 172(1), 491–493. <https://doi.org/10.1016/j.jhazmat.2009.07.009>
- Iglewski, B. H. (1996). *Pseudomonas*. In S. Baron (Ed.), *Medical Microbiology* (4th ed.).
- Kalwarczyk, T., Tabaka, M., & Holyst, R. (2012). Biologistics-Diffusion coefficients for complete proteome of *Escherichia coli*. *Bioinformatics*, 28(22), 2971–2978. <https://doi.org/10.1093/bioinformatics/bts537>
- Kollmann, M., & Sourjik, V. (2007). In Silico Biology: From Simulation to Understanding. *Current Biology*, 17(4). <https://doi.org/10.1016/j.cub.2006.12.034>
- Krzyściak, W., Kościelniak, D., Papież, M., Jurczak, A., & Vyhouckaya, P. (2017). Methods of Biotyping of *Streptococcus mutans* Species with the Routine Test as a Prognostic Value in Early Childhood Caries. *Evidence-Based Complementary and Alternative Medicine*, 2017. <https://doi.org/10.1155/2017/6859543>
- Kuhnert, P., & Christensen, H. (2008). Pasteurellaceae: biology, genomics and molecular aspects. *Kuhnert, Peter; Christensen, Henrik (Eds.) (2008). Pasteurellaceae: Biology, Genomics and Molecular Aspects [Edited Textbook] . Norfolk, UK: Caister Academic Press, 267.*
- Kusters, J. G., van Vliet, A. H. M., & Kuipers, E. J. (2006). Pathogenesis of *Helicobacter pylori* Infection. *Clinical Microbiology Reviews*, 19(3), 449–490.
- Larimer, F. W., Chain, P., Hauser, L., Lamerdin, J., Malfatti, S., Do, L., Land, M. L., Pelletier, D. A., Beatty, J. T., Lang, A. S., Tabita, F. R., Gibson, J. L., Hanson, T. E., Bobst, C., Torres Y Torres, J. L., Peres, C., Harrison, F. H., Gibson, J., & Harwood, C. S. (2004). Complete genome sequence of the metabolically versatile photosynthetic bacterium *Rhodospseudomonas palustris*. *Nature Biotechnology*, 22(1), 55–61. <https://doi.org/10.1038/nbt923>
- Lazdunski, A. M., Ventre, I., & Sturgis, J. N. (2004). Regulatory circuits and communication in gram-negative bacteria. *Nature Reviews Microbiology*, 2(7), 581–592. <https://doi.org/10.1038/nrmicro924>
- Le, K. Y., & Otto, M. (2015). Quorum-sensing regulation in staphylococci-an overview. *Frontiers in Microbiology*, 6(OCT). <https://doi.org/10.3389/fmicb.2015.01174>

- Lenchenko, E., Blumenkrants, D., Sachivkina, N., Shadrova, N., & Ibragimova, A. (2020). Morphological and adhesive properties of *Klebsiella pneumoniae* biofilms. *Veterinary World*, *13*(1), 197–200. <https://doi.org/10.14202/vetworld.2020.197-200>
- Li, H., Li, X., Wang, Z., Fu, Y., Ai, Q., Dong, Y., & Yu, J. (2015). Autoinducer-2 regulates *Pseudomonas aeruginosa* PAO1 biofilm formation and virulence production in a dose-dependent manner. *BMC Microbiology*, *15*(1). <https://doi.org/10.1186/s12866-015-0529-y>
- Li, Y. H., Tang, N., Aspiras, M. B., Lau, P. C. Y., Lee, J. H., Ellen, R. P., & Cvitkovitch, D. G. (2002). A quorum-sensing signaling system essential for genetic competence in *Streptococcus mutans* is involved in biofilm formation. *Journal of Bacteriology*, *184*(10), 2699–2708. <https://doi.org/10.1128/JB.184.10.2699-2708.2002>
- Little, B. J., & Lee, J. S. (2014). Microbiologically influenced corrosion: An update. *International Materials Reviews*, *59*(7), 384–393. <https://doi.org/10.1179/1743280414Y.0000000035>
- Liu, B., Yi, L., Li, J., Wang, Y., Mao, C., & Wang, Y. (2020). Autoinducer-2 influences tetracycline resistance in *Streptococcus suis* by regulating the tet(M) gene via transposon Tn916. *Research in Veterinary Science*, *128*, 269–274. <https://doi.org/10.1016/j.rvsc.2019.12.007>
- Liu, L., Li, F., Xu, L., Wang, J., Li, M., Yuan, J., Wang, H., Yang, R., & Li, B. (2020). Cyclic AMP-CRP Modulates the Cell Morphology of *Klebsiella pneumoniae* in High-Glucose Environment. *Frontiers in Microbiology*, *10*. <https://doi.org/10.3389/fmicb.2019.02984>
- Lu, Z., Guo, W., & Liu, C. (2018). Isolation, identification and characterization of novel bacillus subtilis. *Journal of Veterinary Medical Science*, *80*(3), 427–433. <https://doi.org/10.1292/jvms.16-0572>
- Luke, S., Cioffi-Revilla, C., Panait, L., Sullivan, K., & Balan, G. (2005). MASON: A Multiagent Simulation Environment. *Simulation*, *81*(7), 517–527. <https://doi.org/10.1177/0037549705058073>
- Lynch, M. J., Swift, S., Kirke, D. F., Keevil, C. W., Dodd, C. E. R., & Williams, P. (2002). The regulation of biofilm development by quorum sensing in *Aeromonas hydrophila*. *Environmental Microbiology*, *4*(1), 18–28. <https://doi.org/10.1046/j.1462-2920.2002.00264.x>
- Macal, C. M., & North, M. J. (2010). Tutorial on agent-based modelling and simulation. In *Journal of Simulation* (Vol. 4, Issue 3, pp. 151–162). <https://doi.org/10.1057/jos.2010.3>
- Madigan, M. T., Martinko, J. M., & Parker, J. (2015). *Brock biology of micro-organisms*.
- McGuffee, S. R., & Elcock, A. H. (2010). Diffusion, crowding & protein stability in a dynamic molecular model of the bacterial cytoplasm. *PLoS Computational Biology*, *6*(3). <https://doi.org/10.1371/journal.pcbi.1000694>
- MEDSCAPE homepage. (n.d.). Retrieved November 10, 2020, from <https://www.medscape.com/>
- Merritt, J., Qi, F., Goodman, S. D., Anderson, M. H., & Shi, W. (2003). Mutation of luxS affects biofilm

- formation in *Streptococcus mutans*. *Infection and Immunity*, 71(4), 1972–1979.  
<https://doi.org/10.1128/IAI.71.4.1972-1979.2003>
- Microbiology society homepage*. (n.d.). Retrieved November 10, 2020, from  
<https://www.microbiologyresearch.org/>
- Miller, J., Parker, M., Bourret, R. B., & Giddings, M. C. (2010). An agent-based model of signal transduction in bacterial chemotaxis. *PLoS ONE*, 5(5).  
<https://doi.org/10.1371/journal.pone.0009454>
- Miller, M. B., & Bassler, B. L. (2001). Quorum sensing in bacteria. *Annual Review of Microbiology*, 55, 165–199. <https://doi.org/10.1146/annurev.micro.55.1.165>
- Miller, S. C. M., LiPuma, J. J., & Parke, J. L. (2002). Culture-based and non-growth-dependent detection of the *Burkholderia cepacia* complex in soil environments. *Applied and Environmental Microbiology*, 68(8), 3750–3758. <https://doi.org/10.1128/AEM.68.8.3750-3758.2002>
- Monroe, D. (2007). Looking for Chinks in the Armor of Bacterial Biofilms. *PLoS Biology*, 5(11), e307.  
<https://doi.org/10.1371/journal.pbio.0050307.g002>
- Morgan-Sagastume, F., Larsen, P., Nielsen, J. L., & Nielsen, P. H. (2008). Characterization of the loosely attached fraction of activated sludge bacteria. *Water Research*, 42(4–5), 843–854.  
<https://doi.org/10.1016/j.watres.2007.08.026>
- MR, P., & EP, G. (2005). Sociomicrobiology: the connections between quorum sensing and biofilms. *Trends in Microbiology*, 13, 27.
- Murray, P. R., Rosenthal, K. S., & Pfaller, M. A. (2009). *Medical microbiology*.  
<https://www.elsevier.com/books/medical-microbiology/murray/978-0-323-29956-5>
- Neumann, A., Patzelt, D., Wagner-Döbler, I., & Schulz, S. (2013). Identification of new N-acylhomoserine lactone signalling compounds of *Dinoroseobacter shibae* DFL-12T by overexpression of *luxI* genes. *ChemBioChem*, 14(17), 2355–2361.  
<https://doi.org/10.1002/cbic.201300424>
- Noid, W. G. (2013). Perspective: Coarse-grained models for biomolecular systems. *Journal of Chemical Physics*, 139(9). <https://doi.org/10.1063/1.4818908>
- O'Rourke, J., & Bode, G. (2014). Morphology and Ultrastructure. In *Helicobacter pylori* (pp. 53–67).  
<https://doi.org/10.1128/9781555818005.ch6>
- Pereira, C. S., Thompson, J. A., & Xavier, K. B. (2013). AI-2-mediated signalling in bacteria. *FEMS Microbiology Reviews*, 37(2), 156–181. <https://doi.org/10.1111/j.1574-6976.2012.00345.x>
- Pérez-Rodríguez, G., Dias, S., Pérez-Pérez, M., Fdez-Riverola, F., Azevedo, N. F., & Lourenço, A. (2018). Agent-based model of diffusion of N-acyl homoserine lactones in a multicellular

- environment of *Pseudomonas aeruginosa* and *Candida albicans*. *Biofouling*, *34*(3), 335–345.  
<https://doi.org/10.1080/08927014.2018.1440392>
- Pérez-Rodríguez, G., Gameiro, D., Pérez-Pérez, M., Lourenço, A., & Azevedo, N. (2016). Single Molecule Simulation of Diffusion and Enzyme Kinetics. *The Journal of Physical Chemistry B*, *120*(16), 3809–3820. <https://doi.org/10.1021/acs.jpcc.5b12544.s003>
- Pérez-Rodríguez, G., Pérez-Pérez, M., Glez-Peña, D., Fdez-Riverola, F., Azevedo, N. F., & Lourenço, A. (2015). Agent-based spatiotemporal simulation of biomolecular systems within the open source MASON framework. *BioMed Research International*, *2015*.  
<https://doi.org/10.1155/2015/769471>
- Pérez-Velázquez, J., Gölgeli, M., & García-Contreras, R. (2016). Mathematical Modelling of Bacterial Quorum Sensing: A Review. *Bulletin of Mathematical Biology*, *78*(8), 1585–1639.  
<https://doi.org/10.1007/s11538-016-0160-6>
- Perombelon, & Michael, C. M. (1992). *The Prokaryotes* (2nd ed.).
- Rao, R., Karthika, R., Singh, S., Shashikala, P., Kanungo, R., Jayachandran, S., & Prashanth, K. (2008). Correlation between biofilm production and multiple drug resistance in imipenem resistant clinical isolates of *Acinetobacter baumannii*. *Indian Journal of Medical Microbiology*, *26*(4), 333–337. <https://doi.org/10.4103/0255-0857.43566>
- Ray, P., Sharma, J., Marak, R. S. K., Singhi, S., Taneja, N., Garg, R. K., & Sharma, M. (2004). *Chromobacterium violaceum* septicaemia from north India. *Indian Journal of Medical Research*, *120*(6), 523–526.
- Redfield, R. J. (2002). Is quorum sensing a side effect of diffusion sensing? *Trends in Microbiology*, *10*(8), 365–370. [https://doi.org/10.1016/S0966-842X\(02\)02400-9](https://doi.org/10.1016/S0966-842X(02)02400-9)
- Rekha, P. D., Young, C.-C., & Arun, A. B. (2011). Identification of N-acyl-L-homoserine lactones produced by non-pigmented *Chromobacterium aquaticum* CC-SEYA-1T and pigmented *Chromobacterium subtsugae* PRAA4-1T. *3 Biotech*, *1*(4), 239–245.  
<https://doi.org/10.1007/s13205-011-0029-1>
- Reynolds, C. W. (1987). Flocks, herds, and schools: A distributed behavioral model. *Proceedings of the 14th Annual Conference on Computer Graphics and Interactive Techniques, SIGGRAPH 1987*, 25–34. <https://doi.org/10.1145/37401.37406>
- Rubin, L. G. (2018). Other Gram-Negative Coccobacilli. *Principles and Practice of Pediatric Infectious Diseases*, 967-969.e1. <https://doi.org/10.1016/B978-0-323-40181-4.00181-X>
- Ryan, K. J., & Ray, C. G. (2003). *Sherris Medical Microbiology*.  
[http://books.google.co.in/books/about/Sherris\\_Medical\\_Microbiology.html?id=mcjQ96KsQ\\_EC&pgis=1](http://books.google.co.in/books/about/Sherris_Medical_Microbiology.html?id=mcjQ96KsQ_EC&pgis=1)

- Salvadori, G., Junges, R., Åmdal, H. A., Chen, T., Morrison, D. A., & Petersen, F. C. (2018). High-resolution profiles of the *Streptococcus mitis* CSP signaling pathway reveal core and strain-specific regulated genes. *BMC Genomics*, *19*(1). <https://doi.org/10.1186/s12864-018-4802-y>
- Schroeder, J. L., Lunn, M., Pinto, A. J., Raskin, L., & Sloan, W. T. (2015). Probabilistic models to describe the dynamics of migrating microbial communities. *PLoS ONE*, *10*(3). <https://doi.org/10.1371/journal.pone.0117221>
- Senadheera, D., & Cvitkovitch, D. G. (2008). Quorum Sensing and Biofilm Formation by *Streptococcus mutans*. In R. Utsumi (Ed.), *Bacterial Signal Transduction: Networks and Drug Targets. Advances in Experimental Medicine and Biology* (631st ed., pp. 178–188). Springer.
- Seviour, T., Hansen, S. H., Yang, L., Yau, Y. H., Wang, V. B., Stenvang, M. R., Christiansen, G., Marsili, E., Givskov, M., Chen, Y., Otzen, D. E., Nielsen, P. H., Geifman-Shochat, S., Kjelleberg, S., & Dueholm, M. S. (2015). Functional amyloids keep quorum sensing molecules in check. *Journal of Biological Chemistry*, *290*(10), 6457–6469.
- Sharma, G., Sharma, S., Sharma, P., Chandola, D., Dang, S., Gupta, S., & Gabrani, R. (2016). *Escherichia coli* biofilm: development and therapeutic strategies. *Journal of Applied Microbiology*, *121*(2), 309–319. <https://doi.org/10.1111/jam.13078>
- Shin, D., Gorgulla, C., Boursier, M. E., Rexrode, N., Brown, E. C., Arthanari, H., Blackwell, H. E., & Nagarajan, R. (2019). N-Acyl Homoserine Lactone Analog Modulators of the *Pseudomonas aeruginosa* RhlI Quorum Sensing Signal Synthase. *ACS Chemical Biology*, *14*(10), 2305–2314. <https://doi.org/10.1021/acscchembio.9b00671>
- Shirliff, M., & Leid, J. (2009). *The Role of Biofilms in Device-Related Infections*.
- Simmons, J., & Gibson, S. (2012). Bacterial and Mycotic Diseases of Nonhuman Primates. *Nonhuman Primates in Biomedical Research*, 105–172. <https://doi.org/10.1016/B978-0-12-381366-4.00002-X>
- Singer, S. W., Erickson, B. K., Verberkmoes, N. C., Hwang, M., Shah, M. B., Hettich, R. L., Banfield, J. F., & Thelen, M. P. (2010). Posttranslational modification and sequence variation of redox-active proteins correlate with biofilm life cycle in natural microbial communities. *ISME Journal*, *4*(11), 1398–1409. <https://doi.org/10.1038/ismej.2010.64>
- Smith, E. F., & Townsend, C. O. (1907). A plant-tumor of bacterial origin. *Science*, *25*(643), 671–673. <https://doi.org/10.1126/science.25.643.671>
- Song, S., Du, L., Yu, J., Ai, Q., Pan, Y., Fu, Y., & Wang, Z. (2015). Does *Streptococcus mitis*, a neonatal oropharyngeal bacterium, influence the pathogenicity of *Pseudomonas aeruginosa*? *Microbes and Infection*, *17*(10), 710–716. <https://doi.org/10.1016/j.micinf.2015.08.001>
- Steidle, A., Allesen-Holm, M., Riedel, K., Berg, G., Givskov, M., Molin, S., & Eberl, L. (2002).

- Identification and characterization of an N-acylhomoserine lactone-dependent quorum-sensing system in *Pseudomonas putida* strain IsoF. *Applied and Environmental Microbiology*, 68(12), 6371–6382. <https://doi.org/10.1128/AEM.68.12.6371-6382.2002>
- Stoodley, P., Sauer, K., Davies, D. G., & Costerton, J. W. (2002). Biofilms as complex differentiated communities. *Annual Review of Microbiology*, 56, 187–209. <https://doi.org/10.1146/annurev.micro.56.012302.160705>
- Sturbelle, R. T., Avila, L. F. da C. de, Roos, T. B., Borchardt, J. L., de Cássia dos Santos da Conceicao, R., Dellagostin, O. A., & Leite, F. P. L. (2015). The role of quorum sensing in *Escherichia coli* (ETEC) virulence factors. *Veterinary Microbiology*, 180(3–4), 245–252. <https://doi.org/10.1016/j.vetmic.2015.08.015>
- Subgingival Microbes. (2015). In *Atlas of Oral Microbiology* (pp. 67–93). <https://doi.org/10.1016/b978-0-12-802234-4.00004-5>
- Szenthe, A., & Page, W. J. (2003). Quorum Sensing in *Agrobacterium tumefaciens* using N-oxo-Acyl-homoserine Lactone chemical signal. In *Tested studies for laboratory teaching* (pp. 145–152). <http://www.zoo.utoronto.ca/able%0Ahttp://www.zoo.utoronto.ca/able/volumes/copyright.htm>
- Todar, K. (2003). *Streptococcus pneumoniae: Pneumococcal pneumonia*. *Todar's Online Textbook of Bacteriology*. <http://textbookofbacteriology.net/S.pneumoniae.html>
- Vendeville, A., Winzer, K., Heurlier, K., Tang, C. M., & Hardie, K. R. (2005). Making “sense” of metabolism: Autoinducer-2, LuxS and pathogenic bacteria. *Nature Reviews Microbiology*, 3(5), 383–396. <https://doi.org/10.1038/nrmicro1146>
- Verbeke, F., De Craemer, S., Debunne, N., Janssens, Y., Wynendaele, E., Van de Wiele, C., & De Spiegeleer, B. (2017). Peptides as quorum sensing molecules: Measurement techniques and obtained levels in vitro and in vivo. *Frontiers in Neuroscience*, 11(APR). <https://doi.org/10.3389/fnins.2017.00183>
- Vilain, S., Luo, Y., Hildreth, M. B., & Brözel, V. S. (2006). Analysis of the life cycle of the soil Saprophyte *Bacillus cereus* in liquid soil extract and in soil. *Applied and Environmental Microbiology*, 72(7), 4970–4977. <https://doi.org/10.1128/AEM.03076-05>
- Wang, Y., Yi, L., Zhang, Z., Fan, H., Cheng, X., & Lu, C. (2014). Biofilm formation, host-cell adherence, and virulence genes regulation of *Streptococcus suis* in response to autoinducer-2 signaling. *Current Microbiology*, 68(5), 575–580. <https://doi.org/10.1007/s00284-013-0509-0>
- Wang, Z., Xiang, Q., Yang, T., Li, L., Yang, J., Li, H., He, Y., Zhang, Y., Lu, Q., & Yu, J. (2016). Autoinducer-2 of *Streptococcus mitis* as a target molecule to inhibit pathogenic multi-species

- biofilm formation in vitro and in an endotracheal intubation rat model. *Frontiers in Microbiology*, 7(FEB). <https://doi.org/10.3389/fmicb.2016.00088>
- Waters, C. M., & Bassler, B. L. (2005). Quorum sensing: Cell-to-cell communication in bacteria. *Annual Review of Cell and Developmental Biology*, 21, 319–346. <https://doi.org/10.1146/annurev.cellbio.21.012704.131001>
- Weber, M., & Buceta, J. (2013). Dynamics of the quorum sensing switch: Stochastic and non-stationary effects. *BMC Systems Biology*, 7. <https://doi.org/10.1186/1752-0509-7-6>
- Wingender, J., & Flemming, H. C. (2011). Biofilms in drinking water and their role as reservoir for pathogens. *International Journal of Hygiene and Environmental Health*, 214(6), 417–423. <https://doi.org/10.1016/j.ijheh.2011.05.009>
- Wooldridge, M., & Jennings, N. R. (1995). Intelligent agents: Theory and practice. *The Knowledge Engineering Review*, 10(2), 115–152. <https://doi.org/10.1017/S0269888900008122>
- Yadav, M. K. (2018). Role of biofilms in environment pollution and control. In *Microbial Biotechnology* (Vol. 1, pp. 377–398). [https://doi.org/10.1007/978-981-10-6847-8\\_16](https://doi.org/10.1007/978-981-10-6847-8_16)
- Yadav, P., Verma, S., Bauer, R., Kumari, M., Dua, M., Johri, A. K., Yadav, V., & Spellerberg, B. (2020). Deciphering streptococcal biofilms. *Microorganisms*, 8(11), 1–31. <https://doi.org/10.3390/microorganisms8111835>
- Yang, Y., & Tal-Gan, Y. (2019). Exploring the competence stimulating peptide (CSP) N-terminal requirements for effective ComD receptor activation in group1 *Streptococcus pneumoniae*. *Bioorganic Chemistry*, 89. <https://doi.org/10.1016/j.bioorg.2019.102987>
- Yu, A. C. S., Loo, J. F. C., Yu, S., Kong, S. K., & Chan, T. F. (2014). Monitoring bacterial growth using tunable resistive pulse sensing with a pore-based technique. *Applied Microbiology and Biotechnology*, 98(2), 855–862. <https://doi.org/10.1007/s00253-013-5377-9>
- Zan, J., Liu, Y., Fuqua, C., & Hill, R. T. (2014). Acyl-homoserine lactone quorum sensing in the *Roseobacter* clade. *International Journal of Molecular Sciences*, 15(1), 654–669. <https://doi.org/10.3390/ijms15010654>
- Zhang, L., Li, S., Liu, X., Wang, Z., Jiang, M., Wang, R., Xie, L., Liu, Q., Xie, X., Shang, D., Li, M., Wei, Z., Wang, Y., Fan, C., Luo, Z. Q., & Shen, X. (2020). Sensing of autoinducer-2 by functionally distinct receptors in prokaryotes. *Nature Communications*, 11(1). <https://doi.org/10.1038/s41467-020-19243-5>
- Zhao, Y. H., Abraham, M. H., & Zissimos, A. M. (2003). Fast calculation of van der Waals volume as a sum of atomic and bond contributions and its application to drug compounds. *Journal of Organic Chemistry*, 68(19), 7368–7373. <https://doi.org/10.1021/jo034808o>
- Zhou, X., & Yuqing, L. (Eds.). (2015). Oral Mucosal Microbes. In *Atlas of Oral Microbiology* (pp. 95–

107). Academic Press.



# Annex

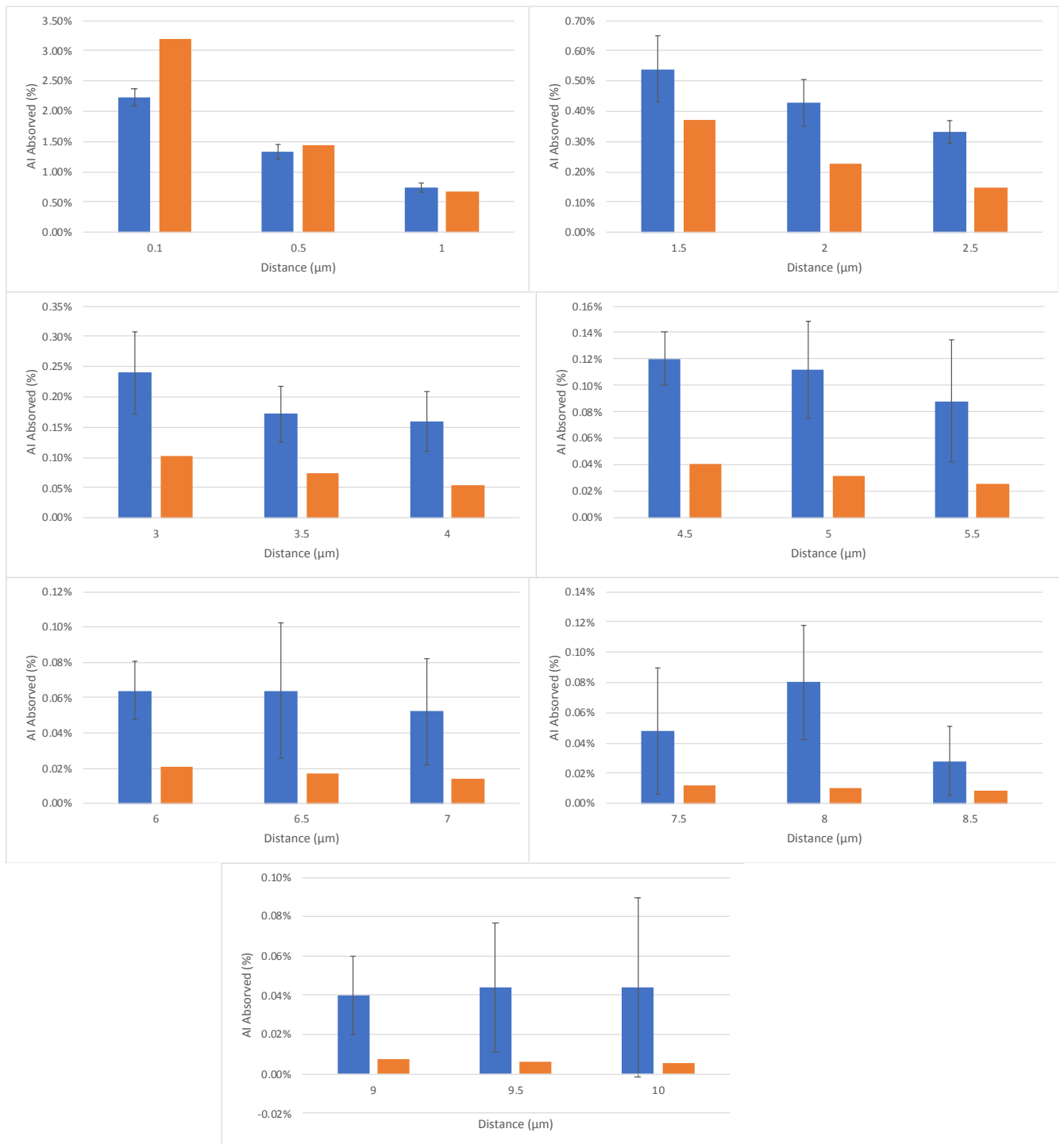


**Figure A 1.** Detailed results for the algebraic approach and simulation tests of *P. aeruginosa* and *S. mitis* when aligned horizontally at different distances, where the former is the one releasing the sensor molecule. In blue is the simulation results and in orange are the results of the mathematical model.

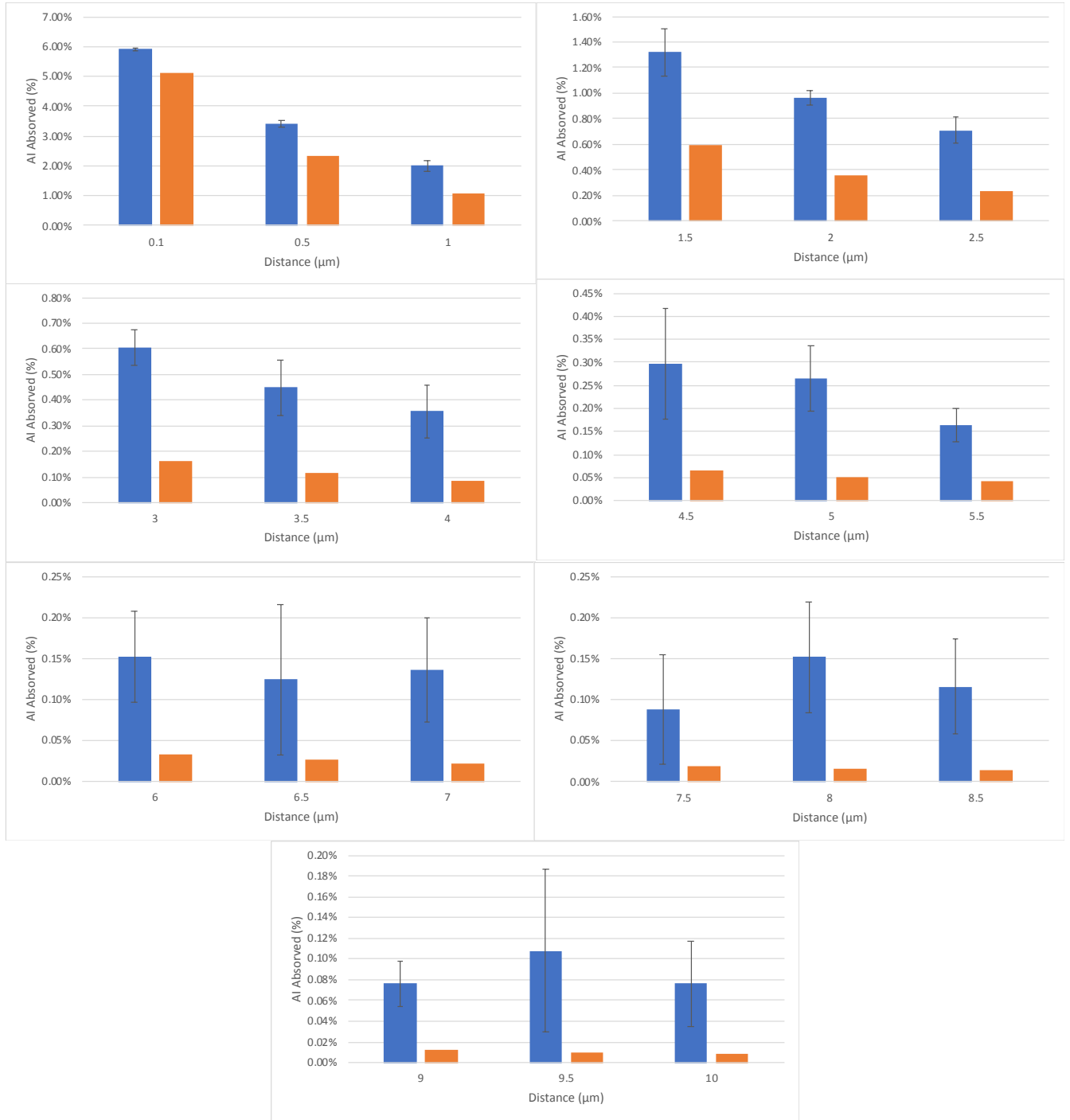


**Figure A 2.** Detailed results for the algebraic approach and simulation tests of *S. mutans* and *S. mitis* at different distances, where the former is the one releasing the sensor molecule. In blue is the simulation results and in orange are the results of the mathematical

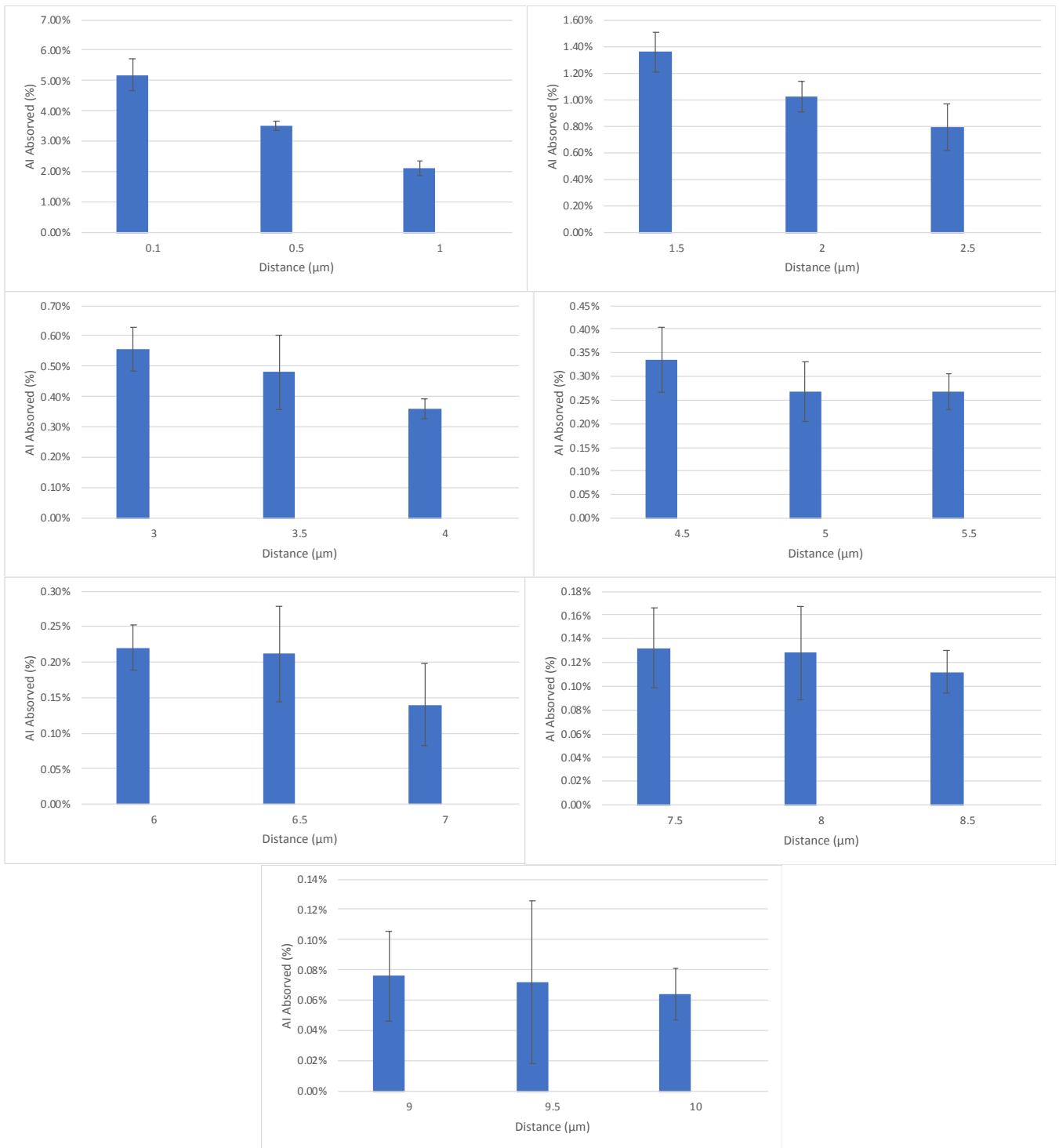


**Figure A 3.** Detailed results for the algebraic approach and simulation tests of *P. aeruginosa* and *S. mitis* when aligned vertically at different distances, where the former is the one releasing the sensor molecule.